AN INFRARED CORONAGRAPHIC SURVEY FOR SUBSTELLAR COMPANIONS

Patrick J. Lowrance,[1] E. E. Becklin,[2] Glenn Schneider,[3] J. Davy Kirkpatrick,[4] Alycia J. Weinberger,[5]
B. Zuckerman,[2] Christophe Dumas,[6] Jean-Luc Beuzit,[7] Phil Plait,[8] Eliot Malumuth,[9]
Sally Heap,[9] Richard J. Terrile,[10] and Dean C. Hines[11]

ABSTRACT

We have used the F160W filter (1.4–1.8 μm) and the coronagraph on the Near-Infrared Camera and Multi-Object Spectrometer (NICMOS) on the *Hubble Space Telescope* to survey 45 single stars with a median age of 0.15 Gyr, an average distance of 30 pc, and an average H magnitude of 7 mag. For the median age we were capable of detecting a $30M_J$ companion at separations between 15 and 200 AU. A $5M_J$ object could have been detected at 30 AU around 36% of our primaries. For several of our targets that were less than 30 Myr old, the lower mass limit was as low as $1M_J$, well into the high mass planet region. Results of the entire survey include the proper-motion verification of five low-mass stellar companions, two brown dwarfs (HR7329B and TWA5B), and one possible brown dwarf binary (Gl 577B/C).

Key word: stars: low-mass, brown dwarfs

1. INTRODUCTION

Just over a decade ago, substellar astronomy exploded in discoveries with the first brown dwarfs in the Pleiades (Rebolo et al. 1995), the first "cool" brown dwarf, Gl 229B (Nakajima et al. 1995), and the first extrasolar planet (Mayor & Queloz 1995). The added identification of hundreds of field brown dwarfs in large-scale surveys such as the Two Micron All Sky Survey (2MASS; Skrutskie et al. 1997) and the Sloan Digital Sky Survey (SDSS; York et al. 2000) led to the creation of two new spectral types, L and T (Kirkpatrick et al. 1999; Burgasser et al. 2002; Geballe et al. 2002).

Brown dwarfs occupy the important region in the mass range between stars and planets. Their existence and properties give insight into stellar and planetary formation. They are thought to form like stars but do not have enough mass to sustain hydrogen fusion. With low temperatures and compact atmospheres different from stars, the lowest mass brown dwarfs should resemble the higher mass giant planets. The observational distinctions between a planet and brown dwarf at the low-mass end have yet to be constructed except that a "planet" should be a companion to a star.

To fully explore the similarities and differences of stellar and planetary formation, the study of brown dwarfs as companions

is essential. Since the brighter primary's age and distance are known, these two properties that are usually uncertain for field brown dwarfs are already established for companions. Therefore, companions can be standards and anchor models, as the multiplicity fraction, separation distribution, and mass ratio distribution of companions provide important hints as to formation mechanisms. Radial velocity surveys find that about 5% of G stars have massive Jupiter planets within 5 AU but that brown dwarfs are rare (<0.1%) at these separations. Even though Gl 229B is a companion to an M star, many earlier companion searches have turned up few discoveries. Closer looks at the younger cluster and field brown dwarfs have found several to be equal-mass binaries (Zapatero Osorio et al. 1997a; Koerner et al. 1999; Reid et al. 2001). About 20% of field L dwarfs have been shown to be binaries with projected separations <20 AU, while closer to 45% of L dwarf companions to stars are actually binaries (Burgasser et al. 2005). The frequency of brown dwarf companions might be dependent on mass and separation (Gizis et al. 2001), but these ideas need a larger sample to be explored.

The primary goal of this survey was the discovery of substellar companions to young, nearby stars. Here we present results from our infrared coronagraphic survey with the Near-Infrared Camera and Multi-Object Spectrometer (NICMOS) on the *Hubble Space Telescope* (*HST*), including follow-up adaptive optics (AO) observations obtained at the Canada-France-Hawaii Telescope (CFHT) and 200 inch (5 m) Hale Telescope and spectra obtained with the Space Telescope Imaging Spectrograph (STIS). Previously, this survey presented TWA 5B, an $\sim 20M_J$ brown dwarf companion (Lowrance et al. 1999, hereafter L99) and HR 7329B, an $\sim 40M_J$ brown dwarf companion (Lowrance et al. 2000, hereafter L00). The full survey results along with six additional discoveries are presented here.

2. DEFINING THE SAMPLE

As part of the *Infrared Space Observatory* (*ISO*) Debris project to detect dust around main-sequence stars, a list of young, nearby stars was assembled. The list was expanded to include young objects selected through techniques including chromospheric activity, the presence of lithium, and space motions as discussed later. Typically, the systems selected were young, single stars within ~ 50 pc of the Sun. Since brown dwarfs are

[1] Spitzer Science Center, California Institute of Technology, MS 220-6, Pasadena, CA 91125; lowrance@ipac.caltech.edu.

[2] Department of Physics and Astronomy, University of California Los Angeles, Box 951547, Los Angeles, CA 90095.

[3] Steward Observatory, University of Arizona, 933 North Cherry Avenue, Tucson, AZ 85721.

[4] Infrared Processing and Analysis Center, California Institute of Technology, 770 South Wilson Avenue, MS 100-22, Pasadena, CA 91125.

[5] Carnegie Institution of Washington, Department of Terrestrial Magnetism, 5241 Broad Branch Road NW, Washington, DC 20015.

[6] European Southern Observatory, Alonso de Cordova 3107, Vitacura, Casilla 19001, Santiago 19, Chile.

[7] Laboratoire d'Astrophysique, Observatoire de Grenoble, 414 Rue de la Piscine, Domaine Universitaire, BP 53, 38041 Grenoble Cedex 09, France.

[8] Department of Physics and Astronomy, Sonoma State University, 1801 East Cotati Avenue, Rohnert Park, CA 94928.

[9] NASA Goddard Space Flight Center, Code 681, Greenbelt, MD 20771.

[10] Jet Propulsion Laboratory, 4800 Oak Grove Drive, MS 183-501 Pasadena, CA 91109.

[11] Space Science Institute, 4750 Walnut Street, Suite 205, Boulder, CO 80301.

TABLE 1
Survey Stars

Primary	Other Names	α (J2000.0)	δ (J2000.0)	H	Spectral Type	D (pc)	b (deg)	Approximate Age (Gyr)
HR 7329	HD 181296	19 22 51.23	−54 25 26.2	5.03	A0 V	47.7*	−26	0.01–0.04
HR 8799	HD 218396	23 07 28.72	+21 08 03.4	5.33	A5 V	39.9*	−36	0.01–0.04
SAO 170610	HD 37484	05 37 39.63	−28 37 34.6	6.38	F3 V	59.5*	+35	0.02–0.1
HD 35850	...	05 27 04.77	−11 54 03.5	5.19	F7 V	26.8*	−24	0.1
HD 209253	...	22 02 32.98	−32 08 01.6	5.53	F6/F7 V	30.1*	−53	0.2–0.3
HD 105	...	00 05 52.56	−41 45 11.5	6.17	G0 V	40.2*	−73	0.1
HD 70573	...	08 22 49.94	+01 51 33.4	7.36	G6 V	32	+21	0.2–0.3
Gl 311	HD 72905	08 39 11.73	+65 01 15.2	4.25	G1 V	14.3*	+36	0.3
Gl 503.2	HD 115043	13 13 37.10	+56 42 30.1	5.45	G2 V	25.7*	+60	0.3
HD 102982	...	11 51 09.14	−51 52 32.3	6.96	G3 V	~42	+10	0.1?
Gl 577	HD 134319	15 05 50.16	+64 02 49.8	6.88	G5 V	44.3*	+47	0.3–0.6
HD 135363	RE 1507+76	15 07 56.24	+76 12 02.4	7.19	G5 V	29.4*	+38	0.1
HD 180445	...	19 18 12.65	−38 23 04.6	6.84	G8 V	41.7*	−21	0.20?
HD 202917	...	21 20 49.95	−53 02 03.0	7.13	G5 V	45.9*	−43	0.04–0.1
HD 220140	V368 Cep	23 19 26.56	+79 00 12.4	5.87	G9 V	19.7*	+17	0.05–0.1
HD 1405	PW And	00 18 20.76	+30 57 22.0	7.35	K2 V	47.9	−31	0.1
RE 0041+34	QT And	00 41 17.26	+34 25 17.7	6.41	K7 V	15.0	−28	0.03
HD 17925	EP Eri	02 52 32.15	−12 46 11.1	4.22	K1 V	10.4*	−58	0.1–0.2
LkHα 264	WY Ari	02 56 37.65	+20 05 36.0	10.14	K3 V	~65	−34	0.01
HD 21703	AK For	03 29 22.88	−24 06 03.1	6.59	K4 V	31.7*	−54	0.1
Gl 174	HD 29697	04 41 18.82	+20 54 05.5	5.75	K3 V	13.5*	−16	0.06
G 88-24	RE 0723+20	07 23 43.68	+20 25 02.5	7.19	K5 V	23.0	+16	0.1
HD 82443	GJ 354.1A	09 32 43.78	+26 59 18.5	5.28	K0 V	17.8*	+46	0.2
HD 82558	GJ 355	09 32 25.87	−11 11 04.8	6.03	K0 V	18.3*	+28	<0.1
TWA 6	...	10 18 28.86	−31 50 03.3	6.89	K7 V	~60	+21	0.01
Gl 517	HD 118100	13 34 43.19	−08 20 31.3	6.46	K5 V	19.8*	+53	0.05
HD 160934	...	17 38 39.81	+61 14 14.0	7.21	K8 V	24.5*	+32	0.1
HD 177996	SAO 229520	19 08 50.45	−42 25 41.5	5.97	K1 V	31.8*	−21	0.5
HD 197890	BO Mic	20 47 44.97	−36 35 40.7	7.68	K0 V	44.4*	−38	0.1
G 145-43	RE 2131+23	21 31 01.50	+23 20 06.2	6.16	K5 V	25.1*	−20	0.1
Gl 879	HD 216803	22 56 24.08	−31 33 56.1	3.78	K4 V	7.6*	−64	0.2
PS 176	...	01 19 27.34	−26 21 55.3	8.6	M3	25.5	−83	0.1
Gl 207.1	G 99-17	05 33 45.12	+01 56 47.0	7.44	M2.5	14.6	−16	0.1
LH 2026	LP 605-23	08 32 30.28	−01 34 31.1	11.48	M6	19.7	+21	0.1
Gl 354.1B	...	09 32 48.48	+26 59 44.7	8.86	M5.5 V	~18	+46	0.2
TWA 7	...	10 42 30.36	−33 40 17.9	7.44	M4 V	~60	+22	0.01
LH 2320	G 44-43	10 52 15.09	+05 55 10.0	8.21	M5	9.9	+55	0.1
LP 263−64	...	11 03 10.21	+36 39 07.3	9.03	M3.5	23.3	+65	0.1
Steph 932	...	11 15 54.37	+55 19 51.0	6.49	M0.5 V	15.0	+57	0.1
TWA 5	CD −33 7795	11 31 55.40	−34 36 27.3	7.35	M3 V	~60	+25	0.01
TWA 8B	...	11 32 41.37	−26 52 08.8	9.38	M3	~60	+32	0.01
TWA 10	...	12 35 04.48	−41 36 39.9	8.43	M3	~60	+21	0.01
LP 390−16	...	18 13 06.37	+26 01 51.8	9.10	M4	16.6	+19	0.1
Gl 875.1	LH 3861	22 51 52.87	+31 45 16.6	7.42	M3.5 V	14.2*	−25	0.3
GJ 1285	AF Psc	23 31 44.81	−02 44 39.7	10.85	M4	29.2	−59	0.1

Notes.—This table was constructed through extensive use of the SIMBAD database. D is distance, and b is Galactic latitude. Asterisks denote *Hipparcos*-determined distances. TWA star distances are based on cluster membership; otherwise, distances are photometric. Units of right ascension are hours, minutes, and seconds, and units of declination are degrees, arcminutes, and arcseconds.

relatively dim, younger and closer ones should be brighter and therefore easier to detect.

Brown dwarfs and giant planets are more luminous when they are young because of gravitational contraction energy remaining from formation. Models of substellar objects show that $L \sim t^{-1.3} M^{2.24}$, where L is luminosity, t is age, and M is mass, based on cooling curves using atmospheric physics (Burrows et al. 1997). Since models predict that the bolometric correction in the H band does not change much for cool temperatures below 3000 K, we can expect a similar relation for an object's H-band flux as a function of mass and age. If atmospheric models are correct, we expect a $5M_J$ object to have an $M_H \sim 17.5$ mag at 10^8 yr (Burrows et al. 1997).

2.1. Building the Target List

As part of the NICMOS Instrument Definition Team (IDT), the Environments of Nearby Stars (EONS) team was awarded guaranteed time of approximately 80 orbits on the *HST*, of which 50 were dedicated to finding brown dwarfs around young stars (*HST* Program IDs 7226 and 7227). The team prioritized the list of stars to the 50 best targets, attempting to maximize the probability of discovery. The three main factors that were taken into account include lack of binarity, close distance, and young age.

A close (<20″) binary significantly lowers the probability of another companion being in a close, stable orbit (within a few
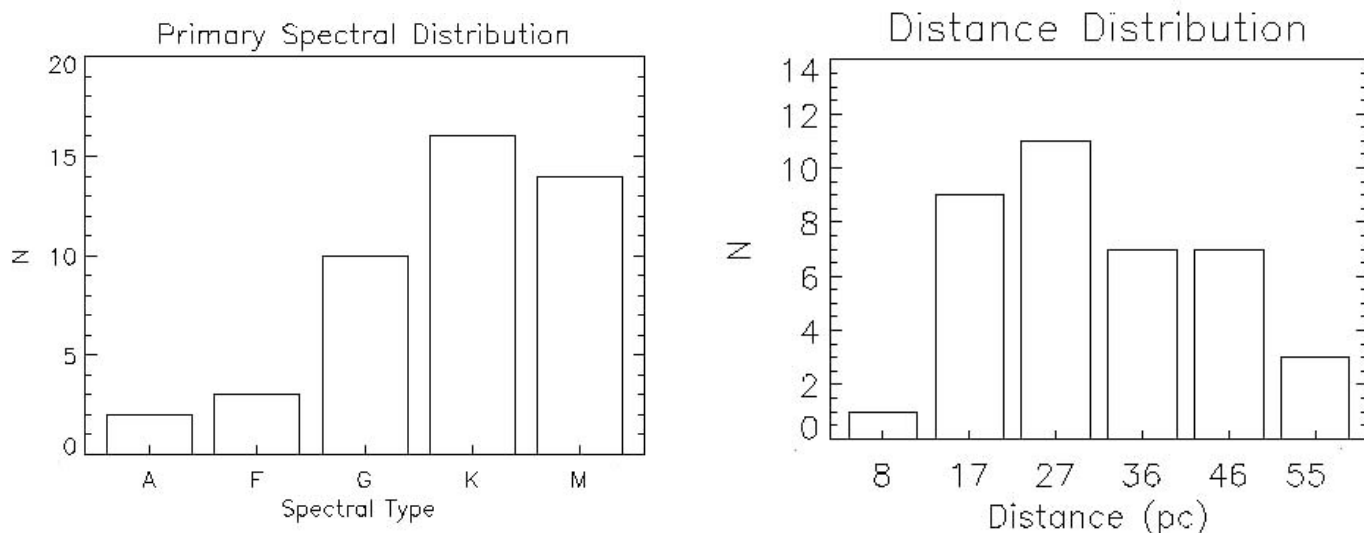
Fig. 1.—Sample consists of a range of spectral types and distances, with a concentration toward lower mass ($<1.0\ M_\odot$) stars at a median distance of about 30 pc. Half of the distances, or 25, were determined using data from the *Hipparcos* mission.

arcseconds) to the star. Triple systems with a ratio of major axes <5 are thought to be unstable (Harrington 1977). All known close binaries were left off the target list but, since many of the apparently single stars had never been observed at high resolution, some stellar binaries were still to be expected.

At a distance of 50 pc, objects discovered at 0″.4 (a coronagraphic radius of 0″.3) would be 20 AU from the primary star. This is near the maximum in distribution of separations of binaries in Duquennoy & Mayor (1991). Most of the distances for the targets are determined from the *Hipparcos* mission data and are accurate to a few percent. Some of the stars were not observed by the *Hipparcos* mission, and the photometric distance is used. The distribution of distances peaks near 30 pc, the median distance of the sample. The minimum observable separation of 12 AU, at 30 pc, is inside the average orbital distance of giant planets in our solar system. A few stars selected for this project were farther than 50 pc but were chosen because of their extreme youth (e.g., the TW Hydrae association).

There are many stars within $\sim$50 pc of the Sun with ages similar to or less than the age of the Pleiades ($t = 125$ Myr; Stauffer et al. 1998). Youth can be inferred observationally in a number of ways. These different age determinations can be intercompared. One method is measuring photospheric lithium abundance in stars later than $\sim$K5 in spectral type. This fragile element is destroyed at temperatures greater than 2×10^6 K, and convective motions within a late-type star's layers will, within less than 100 Myr for 0.1 $M_\odot$ stars, cycle all lithium to the hot core. Studies of stars in clusters (Favata et al. 1993) have shown that at a given spectral type, lithium abundance decreases as a function of age, where age can be determined independently from other means, such as main-sequence fitting.

Another method to determine age is by measuring coronal or chromospheric activity such as Hα emission, Ca H- and K-line emission, and X-ray emission. All of these are coupled to rotational velocity and magnetic field activity, presumably a result of the internal dynamo. Stars typically spin up to high rotational velocities ($>$200 km s^{-1}) when young and slow down as angular momentum is lost through stellar winds. A problem with this method on an individual star basis is that close binaries with periods less than a few weeks are often tidally locked and maintain high levels of activity regardless of age.

Main-sequence fitting is another useful method that places stars on an H-R diagram and compares their location to clusters of approximate ages. Accurate distances of field stars became available as a result of the *Hipparcos* mission, and main-sequence fitting became much more effective in the age determination. One method of age determination is kinematics, in which comparisons are made between a star's Galactic motion and that of clusters of approximate ages. This proves successful in providing a general age group for individual stars.

Age estimates for our sample are found using an intercomparison of lithium abundance, coronal and chromospheric activity, rotational velocity, main-sequence fitting, and kinematics (see the Appendix). Upper limits and lower limits are calibrated against samples of T Tauri stars ($\sim$1 Myr) and stars in young, nearby clusters such as the Pleiades (125 Myr), Ursa Major (300 Myr), and the Hyades (600 Myr).

The original plan was to reobserve all frames containing point sources within 3–4 yr for proper motion confirmation of companionship. However, it was learned after launch that NICMOS would have a shorter lifetime than expected because of coolant problems. Because of this, the chance for follow-up was limited to within 2 yr with NICMOS or from ground-based telescopes. To limit the number of extraneous background stars, we therefore excluded most target stars with $|b| < 15°$.

The final sample (Table 1) consists of 45 single stars with a median distance of 30 pc and a median age of 0.15 Gyr. The sample was concentrated toward cooler spectral types (Fig. 1) mainly for contrast considerations, because faint substellar companions will be easier to detect near fainter primaries. They were observed as scheduled from 1998 March 18 to December 18.

3. OBSERVATIONS

3.1. *Using NICMOS: An Infrared Instrument Aboard the Hubble Space Telescope*

The main problem with trying to image brown dwarfs or giant planets around main-sequence stars is the overwhelming brightness of the primary. A substellar companion will be much fainter than the star it orbits (i.e., a Gl 229B–like object, $L = 2 \times 10^{-5}\ L_\odot$, orbiting a solar-like star of 1 $L_\odot$). The cool brown dwarf makes up a little of this in the infrared, where it radiates much of its light, and is brighter with youth, but the primary is still much brighter.
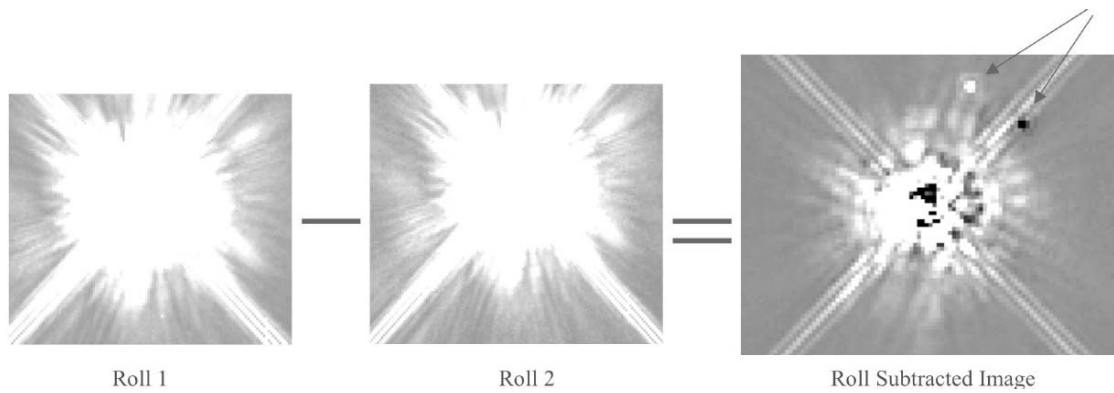
Fig. 2.—Roll subtraction is very effective in eliminating much of the light from the primary star (the example shown is TWA 7). The star was imaged in the coronagraphic hole (*left*), the telescope was rolled by 29°.9, and the star was imaged again (*middle*). Subtraction (*right*) of the two images reveals a stellar-like object approximately 2″ and 10 mag fainter than the primary. (All three images are stretched from −1 to 1 ADU s^{-1} and are approximately 4″ × 4″ around the coronagraph.) The object around TWA 7 was found by follow-up observations to not have the same proper motion as the primary.

According to theory (Burrows et al. 1997), Gl 229B was 50 times, or 4.25 mag, brighter at 10^8 yr old. Also, formation theories of high-mass planets predicted orbits that are very close to the primaries as well, so high resolution, achievable from space, was essential. NICMOS is a second-generation instrument for the *HST* and has three available cameras. Camera 2 has an ∼19″ × 19″ field of view with 0″.076 pixels and provides higher resolution and image stability than ground-based instruments. Most importantly, the coronagraph on camera 2 is actually a hole in the field divider mirror that is baffled with a cold pupil plane mask (Thompson et al. 1998), and therefore it can provide higher sensitivity to faint companions than direct imaging (and point-spread function [PSF] subtraction) because of the actual reduction of light in the optical path.

We conducted the survey at F160W, which corresponds roughly to the *H*-band filter on the ground. There are three main reasons for choosing this filter. First, the dominant sources of background radiation are the zodiacal light at short wavelengths and the thermal background emission from the telescope at long wavelengths. The sum of these two components are a minimum at 1.6 μm (see Table 4.8 of the NICMOS Data Handbook). Second, in camera 2 the PSF is Nyquist sampled at 1.67 μm, and ∼90% of the light of the primary is contained within the coronagraph, which has a 0″.6 diameter. Because the coronagraphic hole was baffled, it reduced the amount of light from the primary by a factor of 6 at 1″ compared to direct imaging (Schneider 1998). Finally, there are two main filters on camera 2 that could have been used, F165M (1.55–1.75 μm) and F160W (1.4–1.8 μm). There was a question about which of these would be more useful in detecting very cool objects ($T < 1000$ K) because of the presence of methane absorption in the *H* band. Using the spectrum of Gl 229B, a comparison of the filters found that an object with a similar flux and temperature would have a 1.6 times greater signal-to-noise ratio in the wider filter. Therefore, we conducted our imaging survey on camera 2 with the coronagraph at F160W.

In target acquisition the centroid of the target's PSF is placed at the "low scatter point" of the hole by an onboard acquisition. It is slightly different from the center (−0.75 pixels in the *x*-direction and −0.25 pixels in the *y*-direction) to optimize stray light rejection determined by in-flight testing of the NICMOS IDT (Schneider et al. 2001). Our choice of this placement point within the coronagraphic hole was designed to reduce the intensity of the speckle pattern from the optics at the edge of the hole.

With the target behind the coronagraph, we reduced the amount of light in an azimuthal average at the edge of the coronagraph compared to direct imaging, allowing for a deeper investigation for companions. We developed an observing strategy to go even deeper, as explained below.

3.2. *Roll Subtraction*

HST has the ability to slew in three ways: in *x*, in *y*, and in θ. In order to keep the target star in the same position behind the coronagraph, as well as to simplify the removal of the stellar profile, we designed two observations of the star at different spacecraft orientations ($\delta\theta$) separated by 29°.9.[12] This was the maximum roll the telescope could maintain and still keep its solar arrays pointed toward the Sun. For a companion 0″.5 from the star, a 26° roll is the minimum needed for the two PSFs (the companion's PSF at the two roll angles) to be separated by a distance equal to their first Airy maxima. Therefore, the observing strategy is to place the star behind the coronagraph, observe for about 800 s, roll the telescope, and observe again for 800 s. This integration time fit both rolls into one orbit, allowing for the roll and second target acquisition. Actual integration times per observation varied from 42 to 256 s depending on the brightness of the primary (saturation at 0″.4 was avoided) with multiple frames adding up to ∼800 s. The 800 s was typically split into at least three MULTIACCUM (nondestructive read) integrations (MacKenty et al. 1997).

This helped reduce intrinsic detector nonlinearities and lessened the chance of saturating pixels at small angular distances from the occulted core of the target PSF. It also made maximum use of the available dynamic range. When we subtract the two images, the background from the star should ideally subtract out, and if there are any objects in the field, two images of each should remain (Fig. 2). Because of thermally induced changes in the telescope (or "breathing") the *HST*+NICMOS PSF varies on close to an orbit timescale (even slightly within an orbit) and so scattered light residuals persist as the 10% of the light not contained in the coronagraph will change slightly (Schneider et al. 2001). Therefore, observing at two rolls within an orbit minimized these changes.

3.3. *Reduction of NICMOS Data*

The NICMOS coronagraphic images were independently reduced and processed utilizing calibration darks and flat fields

---

[12] A few observations were made at $\delta\theta < 29°.9$ because of the lack of sufficient guide stars at both orientations.

created by the NICMOS IDT from on-orbit observations rather than library reference files prepared by the Space Telescope Science Institute (STScI). Mainly, flat fields were augmented with renormalized data from contemporaneous lamp calibration images (obtained as part of the acquisition process) to help remove artificial edge gradients and allow for calibration directly around the coronagraphic hole (Schneider 2002). Using the NICRED program (McLeod 1997), the observations were bias- and dark-subtracted, corrected for nonlinearities using the ramp of the MULTIACCUM imaging mode, and flat-fielded. Bad pixels were masked in the calibration steps and replaced with values interpolated from neighboring pixels with a cubic spline function. The three calibrated images at each orientation were then averaged to create final images.

As a final step, the cleaned calibrated images from each of the two spacecraft orientations were subtracted from each other, leaving lower amplitude residual noise near the coronagraphic hole edge, as well as positive and negative conjugates of any objects in the field of view (Fig. 2). Registration of the images was done "by eye" for the smallest residuals as the second image's position was changed by 0.05 pixel in the x- and y-directions. It was found early on that the diffraction spikes were never quite aligned in the best azimuthal subtraction, and "by eye" ultimately led to the best subtraction. A significant component of the residuals in the diffraction spikes arise in a small misalignment of the image of the mirror support structure formed in the pupil plane and small shifts of the pupil mask itself over time, inducing a diffraction of the spikes themselves (Schneider et al. 2001). The difference image, therefore, produces a "triple" diffraction spike that varies in amplitude and phase but has nothing to do with the centering of the object in the coronagraph.

Since the target star is occulted in the coronagraphic images, its position to measure offsets of possible companions must be ascertained indirectly. First, the target's position was found in the acquisition image by a least-squares isophotal-ellipse fitting process around the PSF core with a radius of 7 pixels to exclude flux from any close objects. The target placement in the coronagraphic frames was then determined by applying the target-slew vectors used by NICMOS, accessible from the *HST* engineering telemetry, resulting in independent measurements of each offset and position from both orientations.

4. POINT-SOURCE DETECTION

4.1. *Determining Detection Limits*

For a full analysis of the results, it is necessary to determine sensitivity to point sources. To determine the limits at which sources could be detected within the NICMOS roll-subtracted images of the observed stars, we planted[13] PSF stars, generated with Tiny Tim (Krist & Hook 1997), at random locations in every image. These PSF stars are noiseless and can be adjusted in flux. We examined a range of magnitudes, $H = 10-22$ mag, stepped by 0.2 mag, for each roll subtraction. For each magnitude, 25 stars were planted randomly within $3''$ of the center of the primary. This number of stars was chosen to avoid confusion between planted PSFs. For better statistics, it was repeated 40 times for a total of 1000 planted PSFs at each magnitude. Each of the 40 images was cross-correlated with the Tiny Tim PSF to locate planted sources. The values in the correlation map range from 1 for perfectly correlated points to -1 for perfectly anticorrelated points. The results are then compared with the log of the actual planting,
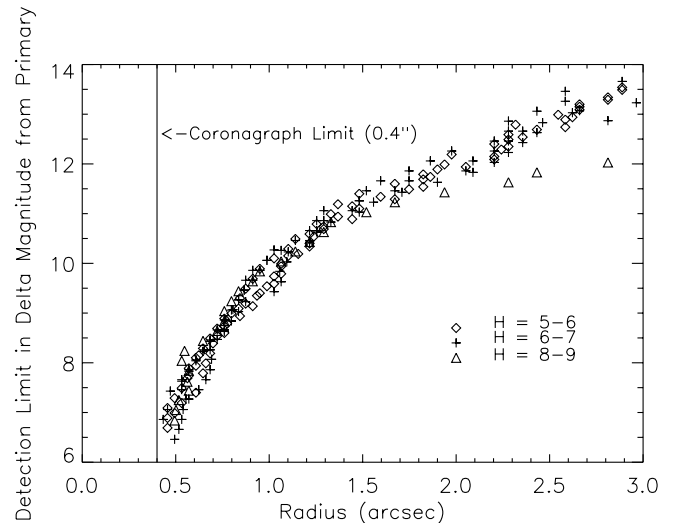

FIG. 3.—Detection limits found by planting and recovering PSF stars in a range of magnitudes within $3''$ of the center of the coronagraph in the roll-subtracted images. Different symbols indicate the different brightnesses of the primary stars plotted.

and the correlation coefficients of the planted stars are recorded, binned, and averaged as a function of radius. Correlation coefficients of 0.9 or above are treated as definite detections. This limit was very conservative, set by the level above which no false hits (glints, etc.) were found for several test images. As a test, two observations with candidate companions in the field were also placed through the routine; one with an $H = 17$ mag ($\Delta m = 9.5$ mag) object at $2''.5$ and one with an $H = 20$ mag ($\Delta m = 13$ mag) object at $2''.5$. The brighter object was found with a correlation of 0.99, while the fainter was found with a correlation of 0.93. The routine found nothing else in each image with a correlation greater than 0.9. The separation from the star at which the correlation reaches 0.9 is then recorded for each magnitude step.

The F160W filter is ~30% wider than ground-based Johnson H-band filters, which necessitates a careful conversion from F160W to the H band for cool-temperature objects. For six M dwarfs between spectral types M6 and M9 with measured F160W and ground-based H-band magnitudes, we find a mean difference of 0.03 mag. Objects with a spectrum like Gl 229B, displaying methane absorption, have an $H-[\mathrm{F160W}]$ color of about 0.2 mag. The quoted H magnitudes of objects less than $80 M_{\mathrm{J}}$ are uncertain by 0.25 mag because of uncertainties in the opacities and gravity dependence of methane absorption (A. Burrows 2001, private communication).

In Figure 3 we plot the detection limits found overall in the observations. Our sample has an average primary magnitude of $H = 7$ mag and a median age of 0.15 Gyr. At $1''$, we can confidently detect a magnitude difference (Δm) of 9.5 mag for all stars. At a median distance of 30 pc, $1'' = 30$ AU and our average limit corresponds to $M_H = 14.1$ mag. From the models of A. Burrows (2001, private communication), this corresponds to less than $20\ M_{\mathrm{J}}$. The most distant stars are the TWA association, in which $1''$ correlates to 50 AU, but they are much younger (10 Myr), so the detection limit is down at a few M_{J}. At $0''.5$, we can detect a Δm of 7 mag, approximately 3 mag better than most speckle imaging programs (i.e., Bouvier et al. 1997; Patience et al. 1998).

This program fully sampled 45 young stars with a median age of 0.15 Gyr with the ability to detect $30 M_{\mathrm{J}}$ brown dwarfs.

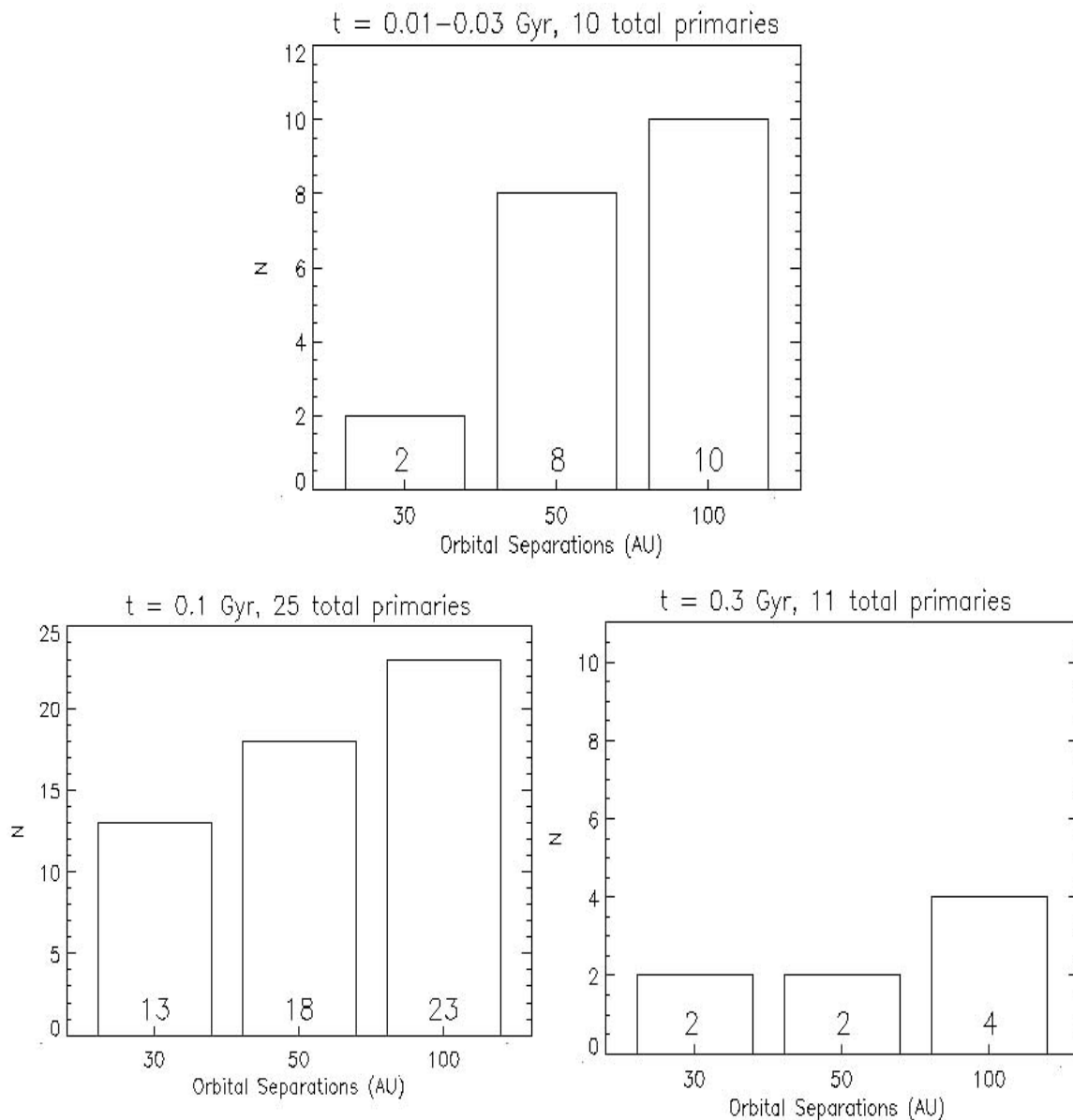[13] Software courtesy of A. Ghez and A. Weinberger.

Fig. 4.—Number of primaries, grouped by age, for which a $5M_J$ object could have been detected at the orbital separations of 30, 50, and 100 AU. Based on the models of A. Burrows (2001, private communication), a $5M_J$ object was assumed to have an absolute H magnitude of 14.2, 16.7, and 18.7 mag at the ages of 0.02, 0.1, and 0.3 Gyr, respectively. This study explored the high mass planet range above $5M_J$ around 36%, 61%, and 80% of the 46 primaries at 30, 50, and 100 AU, respectively.

For several of the younger stars we were able to probe deeper in the mass range to only a few M_J. For the median distance of 30 pc, our search covered 12–120 AU in orbital separation. This covers the maximum of the distribution of companion separations found in the open clusters the Pleiades, Alpha Persei, and Praesepe, the G dwarf radial velocity study, and observations for T Tauri stars (Patience et al. 2002).

4.2. Detectability of High-Mass Planets

At large separations from the primary, we were able to detect objects into the high mass planet range. For our oldest stars, $t = 0.3$ Gyr, a $5M_J$ object is expected to have an absolute H magnitude of 18.7 mag (A. Burrows 2001, private communication). Outside of 5″, for the majority of stars, detection was limited by the sensitivity of the images, [F160W] $\sim$ 22, set by the integration time, so a $5M_J$ object was detectable for primaries at 30 pc. Closer than 5″, detectability depends on the brightness, age, and distance of the primary. Using absolute H magnitudes

of a $5M_J$ object of 14.2, 16.7, and 18.7 mag, at the ages of 0.02, 0.1, and 0.3 Gyr, respectively, we plot the number of primaries in which a detection was possible at separations of 30, 50, and 100 AU (Fig. 4). This survey could have detected a high-mass planet above $5M_J$ around 36%, 61%, and 80% of the 46 primaries at 30, 50, and 100 AU, respectively.

Radial velocity surveys have found $\sim$6% of the over 1000 FGKM stars have high-mass planets within a few AU (Marcy et al. 2004). Since Jovian planets are thought to form at larger distances, several theories have been proposed to explain how these massive planets are so close to their stars. One mechanism proposed (Lin & Ida 1997) is that multiple planets forming within a disk interact gravitationally to kick one planet to an eccentric orbit inside 1 AU, seen in radial velocity studies, while causing another to be ejected to much larger radii (>50 AU).

It is not a strong constraint, but for the 45 stars this program observed, detecting 1–2 high-mass planets at large radii

TABLE 2
Summary of Point-Source Candidates

Primary	H_{prim} (mag)	Spectral Type (primary)	D (pc)	Age (Gyr)	H	Separation[a] (arcsec)	P.A. (deg)	Companion or Background?
HD 102982	6.9	G3 V	42	<0.30	10.9	0.9	28.6	C
LP 390-16	9.10	M4	16.6	0.1	14.4	1.45	226.0	B
Gl 503.2	5.45	G2 V	25.7	0.3	10.5	1.55	354.9	C
TWA 5................................	7.35	M3 V	55	0.01	12.2	1.96	358.8	C
TWA 6................................	6.9	K7 V	55	0.01	19.9	2.54	278.7	B
TWA 7................................	7.4	M4 V	55	0.01	16.8	2.47	142.2	B
HR 7329............................	5.03	A0 V	47.7	0.01–0.04	11.9	4.17	166.8	C
Gl 577	6.88	G5 V	44.3	0.3	10.9	5.34	260.6	C
HD 220140	5.87	G9 V	19.7	0.05	7.8	10.85	216.3	C
Gl 875.1	7.4	M3.5 V	14.2	<0.3	20.2	5.42	250.4	B
HD 160934	7.21	K8 V	24.5	0.1	16.4	8.69	234.8	
					9.67	19.06	151.1	C
HD 180445	6.84	G8 V	41.7	<0.20	9.9	9.45	52.5	C
					20.8	2.88	337.0	
					18.7	4.51	108.3	
					17.8	13.87	275.6	
					21.4	11.61	200.7	
LHS 2320...........................	8.2	M5	9.9	0.1	13.5	14.92	96.9	B
					15.9	15.13	93.6	
RE 0723+20.......................	7.19	K5 V	23.0	0.2	14.6	5.12	322.7	B
					17.7	9.78	277.4	
					17.8	13.85	326.9	
HD 177996	5.97	K1 V	31.8	0.5	19.6	5.20	300.9	B
					15.6	8.08	301.1	
					17.9	12.50	244.2	
Gl 207.1	7.4	M2.5	14.6	0.1	18.0, 17.6	4.1, 4.2	197.4, 199.1	
					17.7	9.7	289.6	
HD 82443	5.28	K0 V	17.8	0.2	16.9	6.86	195.3	
HR 8799.............................	5.33	A5 V	39.9	0.01–0.04	21.6	13.71	15.9	
					20.4	15.68	114.3	
RE 1507+76.......................	7.19	G5 V	29.4	0.1	16.6	17.11	8.3	
HD 202917	7.13	G5 V	45.9	0.1	18.1	13.62	230.1	
HD 17925	4.22	K1 V	10.4	0.1	17.47	15.36	294.6	
LkHα 264..........................	10.14	K3 V	65	0.01	16.8	9.28	220.4	
					21.0	9.51	233.4	
Gl 174	5.75	K3 V	13.5	0.06	19.4	14.43	199.2	
HD 197890	7.68	K0 V	44.4	<0.1	17.7	9.04	20.4	
Gl 354.1B...........................	8.86	M5.5 V	18	0.2	16.51	9.51	317.0	
GJ 1285..............................	10.85	M4	29.2	0.1	14.8	19.04	50.4	

Notes.—If a survey star is not found in this list, then there were no point sources detected in the NICMOS images. D is distance. In the last column, a C means the star is a companion, while a B means it is a background object.

[a] All separations have errors of 0″.08.

would be consistent with all of the radial velocity planets having formed in the interaction method described above. However, it is not possible with the imaging data at a single epoch to distinguish between objects formed in situ or those kicked out.

5. IDENTIFICATION AND ANALYSIS OF POINT SOURCES

In Table 2 we present the point sources identified in the coronagraphic survey. "Stellar-like" candidates are those that have a FWHM between 0″.14 and 0″.18 and usually show an Airy diffraction pattern. The high resolution of the observations makes it easy to distinguish between stars and diffuse background galaxies. Several of the candidate companions have been reobserved for proper motion and spectra to confirm companionship and their possible substellar nature. Many candidates were very close to their primaries and had to be followed up with other space-based observations or AO. In this section we describe the

further observations on the candidates that confirmed their background nature or companionship.

5.1. Observations

5.1.1. STIS

The candidate secondaries around HD 177996, TWA 5, HR 7329, Gl 577, HD 102982, and Gl 503.2 were observed between 2000 March and July with STIS (Program 8176). Each primary was acquired into the $52'' \times 0''.2$ slit and then offset based on the NICMOS astrometric results to place the secondary into the slit. To keep the primary as far out of the slit as possible, we employed a slit position angle so that the line joining the primary and secondary was approximately perpendicular to the slit, thereby minimizing contamination from scattered primary light. Spectral imaging sequences were completed in one orbit per star with the G750M grating in three tilt settings with central wavelengths of 8311, 8825, and 9336 Å (resolution ~0.55 Å). For HR 7329B, HD 177996, Gl 503.2B, and HD 102982B we

integrated for 684, 344, and 310 s at each of the three respective tilt settings, and for Gl 577B and TWA 5B the integration times were 340, 172, and 174 s at each tilt setting, respectively. For TWA 5B and Gl 577B, we obtained flat fields after each set of four spectral images. These were recommended by the STIS team to calibrate the known effects of fringing that appear longward of $\sim$7500 Å. After our first sets of medium-resolution spectra were reduced, the library flats served as well as these contemporaneous flats shortward of $\sim$9000 Å. For the rest of the observing program, we used library flats and no longer took flat fields on-orbit. This allowed more time for integration in the later spectra. At each tilt setting we executed a two-position dither of 0".35 along the slit to allow replacement of bad or hot pixels, and the exposures were split for cosmic-ray removal. Thus, we obtained four spectra at each tilt setting.

5.1.2. CFHT

The Gl 577 and Gl 503.2 systems were observed on 1999 March 4 and 5 UT, and HD 180445 was observed on 2000 November 11 with the CFHT using the AO system PUEO (Rigaut et al. 1998) and its 1024×1024 HgCdTe Hawaii detector, KIR (Hodapp et al. 1994). PUEO delivers diffraction-limited images at near-infrared wavelengths (PSF FWHM of 95, 110, and 140 mas for J, H, and K bands, respectively). KIR is used at the f/20 output focus of PUEO and is sensitive in the [0.7–2.5] μm range. Despite poor meteorological conditions, with cirrus covering most of the sky and an uncorrected seeing varying between 0".9 and 1".5 over the nights, PUEO was able to easily detect the bright companions of HD 180445, Gl 577, and Gl 503.2 in a single exposure of a few seconds. All three systems were imaged in the J and K bands.

After correction for bad pixels and flat-fielding procedures, we subtracted the sky background. For this purpose, a series of images was obtained for each filter by placing the science target near the center of each of the detector quadrants. The images were co-added, and the sky background was derived from the median of this set of four images.

5.1.3. Palomar

The stars Gl 577 and Gl 503.2 were observed on 2000 May 14 UT, and the stars RE 0723+20, Gl 875.1, and Gl 207.1 were observed on 2000 September 26 UT with the 200 inch Hale Telescope at Palomar Observatory using the AO system PALAO and its 1024×1024 HgCdTe Hawaii detector, PHARO (Hayward et al. 2001). The system mounts at the Cassegrain focus and can achieve a resolution of 0".05 at K-band wavelengths. Both the Gl 577 and Gl 503.2 systems were observed at K-band wavelengths, and Gl 577 was additionally observed at H-band wavelengths.

Basic reduction included correction for bad pixels and flat-fielding procedures following the same methods for the Palomar observations. Clouds precluded direct photometric observation against standards. We measured the separations for each observation of the pairs. Using the neutral density filters for the position of the saturating primary when the secondary is not seen might lead to a larger statistical offset.

5.1.4. Keck

The Gl 577 system was observed on 2000 August 12 using the AO system with the slit-viewing camera (SCAM) on NIRSPEC (McLean et al. 1998). The H-band Strehl ratio, as measured on the primary, was 0.16 with FWHM = 0".045 in a 10 s exposure.

Because of the small field of view of the infrared camera ($5'' \times 5''$), the primary and secondary were observed in different frames, but the AO atmospheric corrections were made on the

TABLE 3
PROPER MOTION OF PRIMARY STARS WITH FOLLOW-UP

Star	μ_α (mas yr^{-1})	μ_δ (mas yr^{-1})	References
HD 102982	−0.057	−0.081	1
Gl 503.2	0.112	−0.018	2
Gl 577	−0.121	0.112	2
HD 180445	0.099	−0.093	2
HD 220140	0.201	0.072	2
HD 160934	−0.031	0.059	2
LP 390-16	0.207	−0.036	3
HD 177996	0.023	−0.120	2
RE 0723+20	−0.055	−0.238	4
LHS 2320	−0.673	−0.094	5
Gl 875.1	0.527	−0.050	2
TWA 7	−0.122	−0.029	1
TWA 6	−0.060	−0.020	6

REFERENCES.—(1) Høg et al. 2000; (2) Perryman et al. 1997; (3) Luyten 1979; (4) Montes et al. 2001; (5) Bakos et al. 2002; (6) Webb et al. 1999.

primary during the entire observation. Six H-band images of the secondary pair were obtained in sets of 10 co-additions of 1 s integrations dithered about the array.

5.2. Analysis of Follow-up Observations

5.2.1. Background Objects

Indeed, when searching for companions, not all point sources will be companions. That was true with several of the objects detected in this survey. They are presented here as a time-saving service for future astronomers.

5.2.1.1. Candidate Companion to LP 390-16 Is a Background Object

Analysis of the roll-subtracted, coronagraphic images of LP 390-16 reveal a stellar-like object at a separation of 1".45 $\pm$ 0".08 and a position angle of 226° $\pm$ 1° with a F160W magnitude of 14.4 $\pm$ 0.1 mag.

To determine possible companionship with the primary, the epoch 1954 Palomar Observatory Sky Survey (POSS) digitized plate was examined in which a star (star X) was found located approximately 10" $\pm$ 1" at a position angle of 100° $\pm$ 5° from LP 390-16, or 10" east and 2" south. With a 44 yr baseline, if the two stars are unassociated, then LP 390-16, with a proper motion listed in Table 3, should move approximately 9" east and 1".5 south, leaving a separation of approximately 1".1 at a position angle of 120° if star X is a background star. This is close to the detected point source within the errors of measurement on the POSS plates, and the candidate companion was the only object near this position in the NICMOS images. Therefore, we conclude that the secondary we detect in the NICMOS images is consistent with this same background star. This object is not seen in the second-epoch POSS plates, epoch 1993, which could be due to the current proximity of LP 390-16.

5.2.1.2. Candidate Companion to HD 177996 Is a Background Object

A STIS follow-up observation of the candidate companion of HD 177996 was attempted on 2000 February 27. In the NICMOS image the $H = 19.1$ candidate was located at 5".17 at a position angle of 300°.1. A spectrum of the primary star was obtained, and then at the astrometric offset, a spectrum of the secondary was attempted by HST. No detection of the secondary was made in a total exposure time of 10,906 s with the G750L filter, although the diffraction spikes of the primary are visible at the appropriate separation, indicating that the offset was

performed correctly. HD 177996A has a fairly decent proper motion (Table 3), and the NICMOS detection was almost 2 yr earlier (1998 May 3). The half-width of the STIS slit is 0″.1, so if the candidate companion is a background star, it could easily have been at the edge or out of the slit. We therefore conclude that the object is a background star and not a companion to HD 177996.

5.2.1.3. Candidate Companion to RE 0723+20 Is a Background Object

After the NICMOS observation on 1998 October 20, RE 0723+20 was reobserved on 2000 September 26 with the Palomar AO, and the closest of the point sources was seen and measured to be separated by 5″.4 ± 0″.1 and at a position angle of 326°.4 ± 0°.4. With a proper motion listed in Table 3, an object at the original separation and position angle (Table 2) is expected to be at a separation of 5″.47 and 326° in 23 months if it is merely a background object. We conclude that this object, therefore, is not a companion. The other two point sources seen in the *HST* field of view were outside the Palomar AO field of view.

5.2.1.4. Candidate Companion to LHS 2320 Is a Background Object

On 1998 April 1, one of the point sources was observed at a separation of 14″.92 ± 0″.11 and a position angle of 96°.9 ± 0°.2 from the M5 star LHS 2320. Searching the 2MASS point-source database we find two similar sources at the position of LHS 2320 that were observed on 2000 February 12 and separated by 16″.2. With the change in separation over the 1.8 yr baseline similar to the primary's proper motion (Table 3), no other point sources in the vicinity of similar brightness, and a $J - K = 0.38$ mag color, we conclude that it is most likely a background G star (R.A. $= 10^h52^m15^s.3$, decl. $= +05°55'08''$).

5.2.1.5. Candidate Companion to Gl 875.1 Is a Background Object

After the NICMOS observation on 1998 July 7, Gl 875.1 was reobserved on 2000 September 26 with the Palomar AO, and the point source was measured to be separated by 7″.1 ± 0″.1. With the star's proper motion (Table 3), a background object at the original separation and position angle is expected to be at a separation of 6″.5 and 255° within a time baseline of 23 months. We conclude that this object, therefore, is not a companion.

5.2.1.6. Candidate Companion to TWA 7 Is a Background Object

TWA 7 was observed with the NICMOS coronagraph on 26 March 1998 with a candidate companion at a separation of 2″.44 ± 0″.05 and a position angle of 142°.2 ± 0°.1. TWA 7 was also reobserved on 1998 November 2 (Program 7226) with the NIC 1 (pixel scale = ~0″.043 pixel⁻¹) camera with a medium-band F090M filter (central wavelength: 0.9003 μm, $\Delta\lambda$ = 0.1885 μm). It was observed in a two-position dither with four MULTIACCUM integrations of 64 s taken at each position for a total of 512 s. These were dark-subtracted and flat-fielded using calibrations created by the NICMOS IDT.

The F090M filter is a red *I*-band filter, covering 0.8–1.0 μm. The colors of the possible companion (F090M − F160W = 0.72) are consistent with a mid-K star. The candidate was observed with Keck on 2000 February 20 and had changed separation from the primary from 2″.44 ± 0″.05 to 2″.54 ± 0″.08 over the almost 2 yr baseline. With the change in separation and color, we conclude TWA 7 and the candidate were not associated, in agreement with Neuhäuser et al. (2000a).

5.2.1.7. Candidate Companion to TWA 6 Is a Background Object

A point source ($H = 19.93 \pm 0.08$ mag) was discovered on 1998 May 20 at a separation of 2″.549 ± 0″.011 and a position angle of 278°.7 from the young star TWA 6. The field was re-observed with NICMOS on 2002 June 10. The point source was found to lie at a separation of 2″.356 ± 0″.009 and a position angle of 281°.5 ± 0°.1 from TWA 6. This change over the 4 yr baseline corresponds to (R.A., decl.) = (−52.2, −21.2) mas yr⁻¹. Webb et al. (1999) reported the proper motion of TWA 6 to be (−60, −20) mas yr⁻¹, which makes this change in separation wholly consistent with being a background object and not a companion object.

The field of TWA 6 was reobserved with the NIC 1 camera on 1998 December 9 (Program 7226) with a medium-band F090M filter, and the point source was not detected. We derived an upper limit (3 σ) to the flux of [F090M] = 22.6 mag in the predicted position from the NICMOS images. Using low-temperature models to transform between F090M and the *I* band, we calculated an upper limit of $I - H > 3.3$ for the candidate companion. We conclude that the object is a very red background object, nonetheless.

5.2.2. *Confirmed Companions*

In this section, we discuss several positive confirmations from this survey. Two of the discoveries, TWA 5B and HR 7329B, have already been presented in L99 and L00, respectively. Independent proper-motion confirmations for TWA 5B, HR 7329B, and Gl 577B have been presented in Neuhäuser et al. (2000b), Guenther et al. (2001), and Mugrauer et al. (2004). We present the results of the follow-up observations for TWA 5B and bright point sources around other stars with fairly well-known ages.

5.2.2.1. Bright Companions near HD 180445, HD 220140, and HD 160934

Analysis of the subtracted, target-acquisition images of HD 180445 observed on 1998 August 27 reveal a stellar-like object at a separation of 9″.45 ± 0″.08 and a position angle of 52°.5 ± 0°.5. On 2000 November 11, the point source was reobserved at 9″.5 ± 0″.1 and a position angle of 53°.0 ± 0°.8 in the 0.5 s acquisition image before acquiring HD 180445 behind the coronagraph on CFHT. The proper motion of HD 180445 (Table 3) should have changed the separation in 2 yr by 0″.27 if it was a background object. From the 2MASS database we find a point source at a separation of 9″.47 ± 0″.02 and a position angle of 53°.0 ± 0°.1. From both of the observations and the 2MASS observation, we conclude that this pair is most likely a common proper motion pair within the errors. The 2MASS magnitudes of HD 180445A are $J = 6.99 \pm 0.02$ mag, $H = 6.49 \pm 0.03$ mag, and $K = 6.38 \pm 0.02$ mag, while the magnitudes of HD 180445B are $J = 10.46 \pm 0.04$ mag, $H = 9.88 \pm 0.04$ mag, and $K = 9.69 \pm 0.03$ mag. The $J - K$ color of 0.77 and derived absolute magnitudes are consistent with an early- to mid-M star.

A point source was found at a separation of 10″.85 ± 0″.08 and a position angle of 216°.3 ± 0°.5 from HD 220140 when it was observed with NICMOS on 1998 October 25. From 2MASS observations made on 2000 October 8, one point source was found within a 15″ search. The candidate companion is separated from the primary by 10″.85 ± 0″.08 at a position angle of 215°.15 ± 0°.05. From the listed proper motion of HD 220140 (Table 3) the two should have been separated by 11″.20 at a position angle of 217°.5 during the 2 yr baseline if the point source was a background object. Therefore, the candidate is most likely a proper-motion companion within the errors. The 2MASS magnitudes of HD 220140A are $J = 5.90 \pm 0.02$ mag, $H = 5.51 \pm 0.04$ mag, and $K = 5.40 \pm 0.02$ mag. The magnitudes of HD 220140B are $J = 8.04 \pm 0.02$ mag, $H = 7.39 \pm 0.03$ mag, and $K = 7.20 \pm 0.02$ mag with a $J - K$ color and derived absolute magnitudes consistent with a mid-M star.

Weiss (1991) detected a second object at $20''$ at a position angle of $150°$ from HD 160934 that did not change position angle or separation from 1955 to 1990. From the 2MASS database observation on 1999 May 12, one point source is found at $19\rlap{.}''06$ at a position angle of $151\rlap{.}°1$ from the primary. In the 44 yr baseline, with the proper motion of HD 160934 (Table 3), the separation would have increased by at least $1\rlap{.}''5-2''$ if it was not a companion. The 2MASS magnitudes of the companion are $J = 10.25 \pm 0.02$ mag, $H = 9.67 \pm 0.02$ mag, and $K = 9.42 \pm 0.02$ mag with a $J - K$ color ($J - K = 0.83$ mag) and derived absolute magnitudes consistent of a mid-M star.

5.2.2.2. STIS Spectra of Gl 503.2, Gl 577, TWA 5B, and HD 102982

Observations of four candidates were taken with the STIS instrument to determine whether they were background objects or companions. The STIS spectra were calibrated, averaged, binned to a resolution of ~ 6 Å, and normalized to the flux (in ergs s^{-1} cm^{-2} Å^{-1}) at 8500 Å. We compared the final, total spectra to those of standard low-temperature dwarf star spectra with a resolution of 18 Å, a factor of 3 lower than our STIS spectra (Kirkpatrick et al. 1991, 1997; see Fig. 5). All spectra contain the Na I absorption doublet near 8200 Å, which does not appear in late-type giant stars. The TiO absorption bands at 8450 and 8900 Å are also used to choose the best-fitted standard. As seen in Figure 5, the slopes of the spectra from 8600 to 8850 Å are small and fit the dwarf spectra well. The best fit appears to lie between M4 V and M5 V for Gl 503.2B, at M5 V for HD 102982B, between M5 V and M6 V for Gl 577B, and at M9 V for TWA 5B. (The spectrum for HR 7329B was previously published in L00.) The spectral type derived for TWA 5B is consistent with the photometric spectral type M8.5 $\pm$ 0.5 derived by L99 and Neuhäuser et al. (2000b).
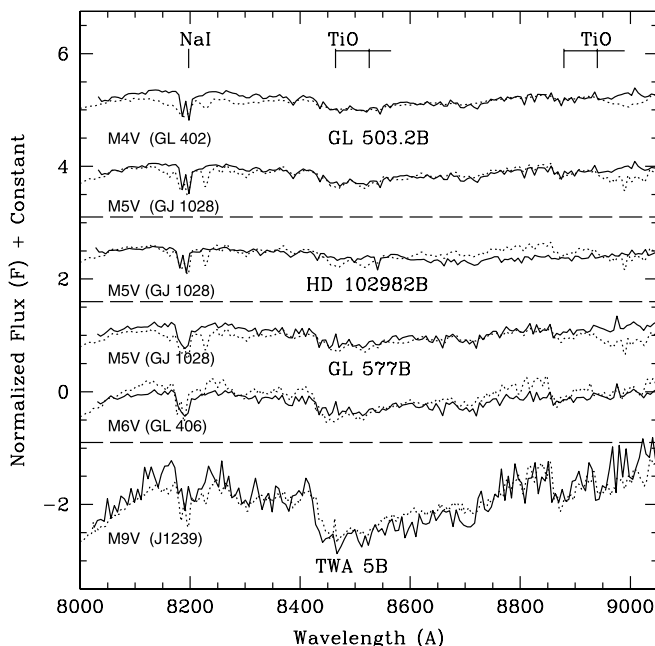

Fig. 6.—Infrared observations of the secondary Gl 577B and C taken with the AO system at Keck. The measured separation is $0\rlap{.}''082$. The orbit can be measured over several years to get dynamical masses for the two components.

5.2.2.3. Binarity of the Companion to Gl 577A

The companion to Gl 577A appears to be elongated in the CFHT images, Palomar, and the NICMOS images, suggesting that the companion is in fact a close binary system itself with an angular separation slightly lower than the instrumental resolution ($\sim$100 mas). The two components were resolved with the Keck system (Fig. 6). The measured separation of $0\rlap{.}''082 \pm 0\rlap{.}''005$ corresponds to a projected radial separation of <4 AU, corresponding to a period of approximately 20 yr. With periodic observations of these two components including radial velocity measurements, the dynamical mass of this low-mass binary can be determined and used to check current evolutionary models.

5.2.2.4. Astrometry of the Companions

From the ground-based observations, a common proper motion between the primaries and secondaries can be established. The known proper motions for the primary stars are listed in Table 3. For the Gl 577 and Gl 503.2 systems, the position of each object was measured in a Gaussian centroid in each reduced image from NICMOS, CFHT, and Palomar. The separations were then calculated and averaged over all measures for each star at each epoch and plotted over time (Fig. 7).

If the secondary is not associated with the primary, then the separation should change in an amount that is calculable from the measured proper motion (Table 3). If Gl 503.2B is not associated with Gl 503.2A, then the separation between them should have changed from $1\rlap{.}''557$ to $1\rlap{.}''613$ from the NICMOS observation until the Palomar observations. Instead, the separation was measured at $1\rlap{.}''579$. This is within the 1 σ error of the NICMOS measure, but it is 3 σ outside of being a background object. We therefore conclude that Gl 503.2B is a likely companion of Gl 503.2A.

Similarly, if Gl 577B and C are not associated with Gl 577A, the separation should have changed from $5\rlap{.}''348$ to $5\rlap{.}''176$ within the 2 yr between observations. The separation was measured to be $5\rlap{.}''31$ in the Palomar observations, 3 σ above the expected change and within 1 σ of the NICMOS measure, leading to the conclusion that Gl 577B and C are indeed companions to Gl 577A.

Fig. 5.—STIS spectra of TWA 5B, Gl 577B, HD 102982B, and Gl 503.2B (solid lines; normalized from ergs s^{-1} cm^{-2} Å^{-1}) separated by the dashed horizontal lines, compared with standard late M-type dwarf spectra (dotted lines; Kirkpatrick et al. 1991, 1997). The zero level of each spectrum is -3.3, -1.4, 0.2, 1.3, 2.7, and 4, respectively, from top to bottom. The best-fitted spectrum was chosen with emphasis on the Na I absorption near 8200 Å and TiO bands near 8450 Å. The best fit appears to lie between M4 V and M5 V for Gl 503.2B, at M5 V for HD 102982B, between M5 V and M6 V for Gl 577B, and at M9 V for TWA 5B. (The longward cutoff of 9050 Å is where the fringing affects the STIS spectrum.)
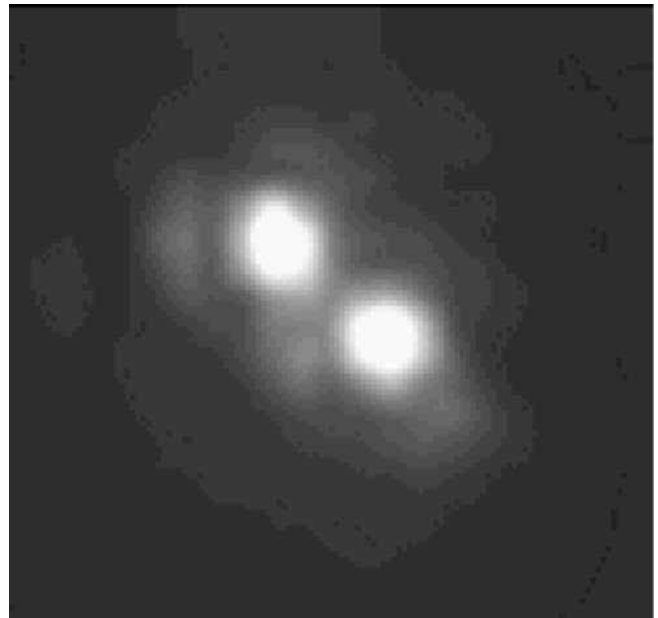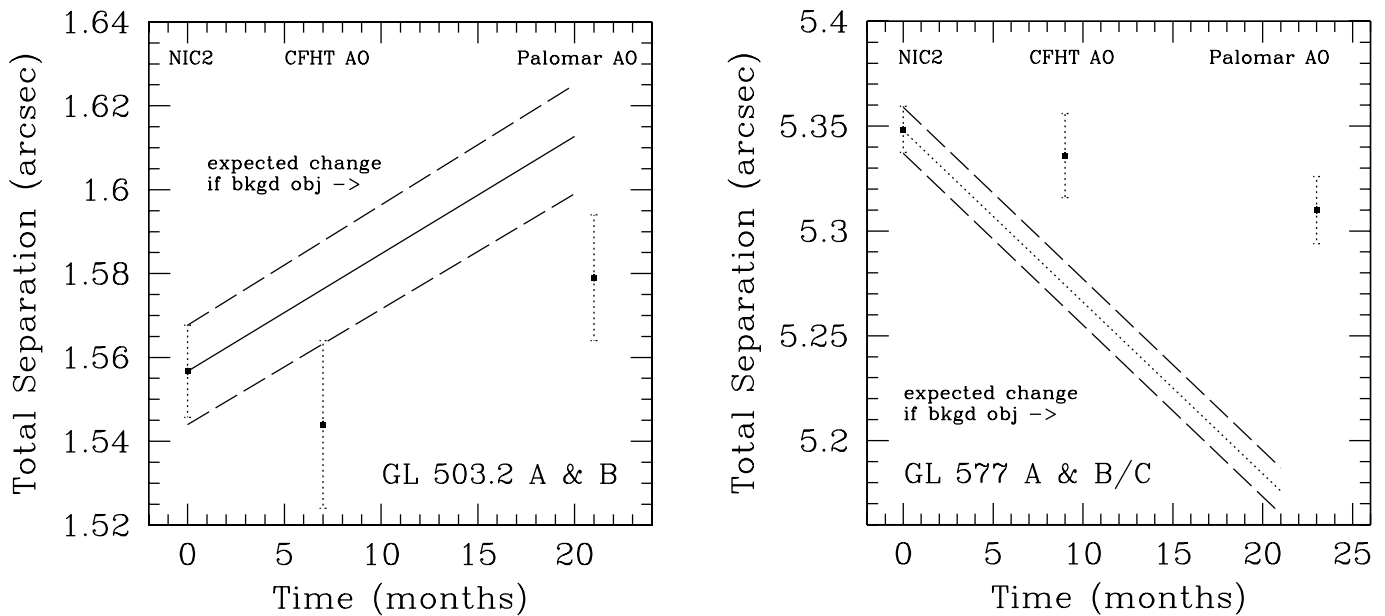
FIG. 7.—Measurements of the separations of two companions (Gl 577B/C and Gl 503.2) made over the last 2 yr are compared to each other, taking into account a 1 σ error bar. The dotted line represents the change in separation expected from the primary's known proper motion if it was not associated with the candidate companion.

The separation of HD 102982A and B was measured with NICMOS and again in the STIS acquisition before being placed in the slit. In the STIS acquisition images, before and after centering, a two-dimensional Gaussian was fitted to get a separation of 0″.943 ± 0″.002. A flux-weighted centroid using the DAOPHOT routine received similar results. The position angle between the two components was calculated to be 28° ± 2°. This is within 1 σ of the separation and position angle measured from the NICMOS image 2.25 yr earlier. The proper motion of the primary should change the separation by 0″.21, or 10 σ, if the B component was not associated; therefore, we conclude that HD 102982B is a companion to HD 102982A.

6. DETERMINATION OF MASS

Mass is the best determinant of the substellar nature of an object. Unfortunately, the current ability to dynamically determine the mass of most of these objects is impossible; therefore, we must rely on evolutionary models of temperature, radius, and luminosity. To plot these objects on evolutionary tracks, we need the luminosity, or absolute magnitude, and the effective temperature. We have converted NICMOS measured photometry to absolute magnitudes using known distances from the primary, and we have used STIS spectra when available, and/or 2MASS infrared colors for the bright companions, to determine spectral type and therefore effective temperatures. Therefore, both parameters on an H-R diagram have been determined independently and have independent errors, which are discussed below.

Proper motion has been demonstrated between the components Gl 577 and HD 102982 in this paper. HR 7329A and B and TWA 5A and B have been confirmed as a proper-motion pair (Guenther et al. 2001; Neuhäuser et al. 2000b). Gl 503.2A and B are likely associated based on the density of background stars and their measured properties. The luminosities or absolute magnitudes of the secondaries have been derived using *Hipparcos* measurements of the primary, which have determined distances known to within a few percent. This small error bar is taken into account when placing companions on the diagrams. The parallactic distance was measured to the primaries by the *Hipparcos* mission (Table 2). With a derived H magnitude

of 10.45 mag for Gl 503.2B and a distance modulus of 2.05, we calculate an absolute H magnitude of 8.38 ± 0.09 mag, with an uncertainty that includes distance errors and NICMOS calibration errors. In a similar manner, we derive an absolute H magnitude of 8.58 ± 0.15 mag for HD 102982B and 7.83 ± 0.09 mag for the Gl 577B and C pair. From the resolved Keck data, we measure a Δm of 0.1 ± 0.1 for the B and C components; therefore, equal-magnitude components will have absolute H magnitudes of 8.58 ± 0.13 mag. The companions to HD 160934, HD 220140, and HD 180445 have absolute magnitudes of 7.72 ± 0.04, 5.92 ± 0.04, and 6.78 ± 0.04 mag, respectively.

6.1. *Effective Temperatures*

The effective temperatures have been determined from the spectra, taken with STIS, from 8000–9000 Å, which have several spectral features including bands of TiO and Na that are specific to low-temperature spectral classes from M4 V to M9 V. The spectral class assignments based on these absorption features are good to 0.5 spectral type, which is the error we assign. Determining the effective temperature adds the largest error, because the relationship between spectral class and effective temperature is largely unknown for late M-type stars. Luhman & Rieke (1998) derive a linear relation based on spectral class from the Leggett et al. (1996) fit to synthetic models, which agrees with the newer models produced by Leggett et al. (1998) within an uncertainty of about 100 K. This relation of Luhman & Rieke (1998) was used to determine the temperatures of our candidates' spectral types, and a 100 K error bar covers a ±0.5 spectral type. We calculate 3180, 3010, and 2840 K for M4 V, M5 V, and M6 V, respectively. For the brightest companions, HD 160934B, HD 180445B, and HD 220140B, we assumed a spectral type of M4 ± 1 from the 2MASS colors and derived absolute magnitudes and get a temperature of 3180 ± 200 K. With the uncertainty for late M-type dwarf star temperatures in mind, we plot the derived temperatures for each spectral class (Fig. 8) with their derived absolute H magnitudes.

6.2. *Derived Mass and Age*

From their placement on pre-main-sequence evolutionary tracks (Baraffe et al. 1998), we can infer a mass for the secondaries
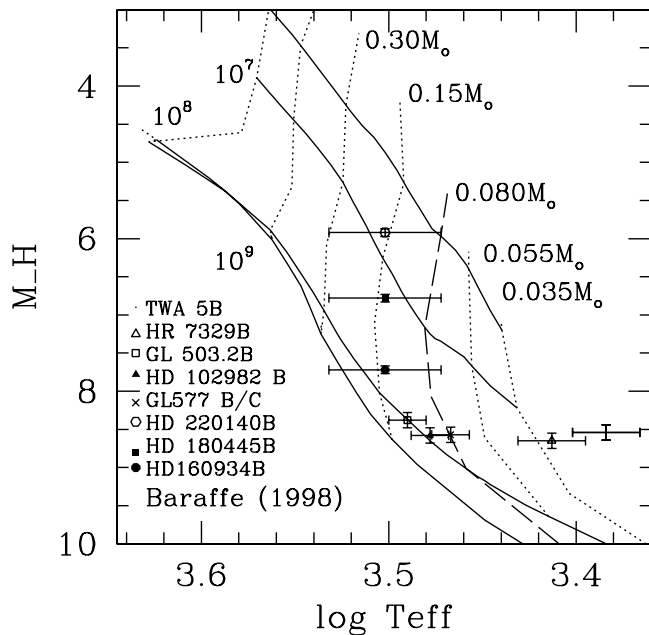
FIG. 8.—H-R diagram of all eight of the discovered companions in this study using the absolute H magnitude determined distances of primary stars and effective temperatures derived from spectra or 2MASS colors. These models (Baraffe et al. 1998) indicate three low-mass stars, two very low mass stars, a binary brown dwarf, and two brown dwarf companions.

(Fig. 8). HD 220140B and HD 160934B seem to be low-mass stars falling near the 10 and 100 Myr isochrones, consistent with the derived ages (discussed in the Appendix) of their primaries. HD 180445B appears to be a young low-mass star near 50 Myr, younger than the derived primary's age, which has an upper limit of 200 Myr, especially since Soderblom et al. (1998b) speculated that it might be a tidally locked binary and not young at all. HD 102982B and Gl 503.2B appear to be consistent with very low mass ($<0.15\ M_\odot$) stars falling on the 100 Myr isochrone with error bars extending between about 70 and 300 Myr. This agrees with ages derived for the primaries from other means. Gl 577B and C appear to lie just on the theoretical brown dwarf mass of $0.08\ M_\odot$ from its infrared magnitude and spectral type at an age of about 70 Myr with error bars extending between 30 and 100 Myr. This has been adjusted by 0.75 mag for being a binary. Since both components are of equal magnitude, this would suggest that both might be high-mass brown dwarfs separated by $\sim$4 AU. The models would also suggest that the Gl 577 system is younger than the Pleiades (100 Myr), supported by the primary's chromospheric activity and rotation. Both HR 7329B and TWA 5B are bona fide brown dwarfs with masses of $30M_J$ and $20M_J$ as previously reported (L99; L00).

7. EXAMINING THE COMPANION MASS FUNCTION

Even though this survey was originally designed to discover brown dwarfs, we can attempt to examine the companion mass function (CMF), and by extension the initial mass function (IMF), across the stellar/substellar border. Since masses can only be accurately determined for close binaries with measurable orbits, to derive appropriate masses we use previously quoted models for the discovered companions. In recent studies of the field (Reid 1999) and the Pleiades (Zapatero Osorio et al. 1997b), the relative number of low-mass stars and brown dwarfs per log mass interval is consistent with being equal, suggesting a flat IMF ($\alpha = 1$) for single stars.

Several caveats exist in any statistical examination of a small size sample. We have only examined a small separation range and thrown out all known binaries within 20″, as mentioned in § 2. Earlier studies in the Pleiades and the field have used hundreds of stars, while we have observed just less than 50, which decreases the statistical significance. With these overall limitations in mind, we first estimate what one might expect in detections for our survey, by dividing the mass range into two logarithmically equal bins, 0.03–0.08 and 0.08–0.2 $M_\odot$. For an approximate idea of how many companions to expect, one can examine statistics within 5 pc of the Sun. Stars less than 0.2 $M_\odot$ make up approximately 24 of 65 stars (37%) within that distance range. Similar statistics are found in the nearest 100 stars taking into account missing systems. For statistics on the separation range of 30–120 AU, one can look at the G dwarf radial velocity survey and find that $\sim$30% of the stars have companions in that separation range (Duquennoy & Mayor 1991).

From these statistics, we might expect 30% of our stars to have companions at the separations available within this study (30–120 AU) and 37% of those companions to be in the 0.08–0.3 $M_\odot$ mass bin. Therefore, we might expect 11% of our 46 star sample, or five companions, in this higher mass bin. This study found companions to HD 180445, HD 220140, HD 160934, Gl 503.2, and HD 102982, which fit that expectation.

For the brown dwarf range (0.03–0.08 $M_\odot$), we have three objects, HR 7329B and Gl 577B and C. For an IMF with an equal mass of stars in equal bins ($\alpha = 2$), we expect about 10 objects in the lower bin, which is not consistent by 3 σ with our observations. For a flat IMF ($\alpha = 1$), one which has an equal number of stars in each mass bin, we expect five objects in the lower mass bin. This is fairly consistent with the findings of this survey, although it leans toward an $\alpha < 1$. Therefore, even with the aforementioned caveats, the CMF we derive from this survey is consistent with the IMF found in the field (Reid 1999) and the Pleiades (Zapatero Osorio et al. 1997b).

8. CONCLUSIONS

In the last decade, the search for substellar objects has achieved spectacular success with the discovery of the first noncontroversial detection of a brown dwarf, the definition of two new spectral types, L and T, and the uncovering of over 500 L and T dwarfs. Even though observations of field dwarfs can answer many questions about formation and fundamental properties, many questions still exist that can only be answered by observations of brown dwarf *companions*. In order to directly detect substellar companions, we developed an infrared coronagraphic survey of young stars with the NICMOS camera on *HST*.

Subtraction of two coronagraphic images taken within the same orbit at two angles of the spacecraft differing by 29°9 was found to produce the most effective method of detecting point sources. For the average primary magnitude of $H = 7$ mag, the survey detected a Δm of 9.5 mag at 1″ with only the subtraction and no other manipulation of the images. This allowed detection into the high mass planet range at 50 AU from over half of the primaries. Results from this survey include five low-mass stars, two brown dwarfs, and one possible binary brown dwarf.

Models play an important role in substellar astronomy, and therefore every substellar companion discovered is extremely important. Because the primaries have been well studied, parameters such as age, distance, and metallicity are known and can be used to provide fiducials to refine the present models. For example, the close binary Gl 577B and C presented in this paper can be reobserved over the next few years to derive a dynamical mass to compare other young substellar field brown

dwarfs. Higher resolution visual and infrared spectra of companions such as TWA 5B and HR 7329B are well constrained with age and metallicity and therefore provide anchors for models. Finally, as more substellar binaries and companions are discovered, the parameters can be used as important pointers toward answering the questions of stellar formation versus substellar formation versus planetary formation.

APPENDIX

INDIVIDUAL TARGET AGES

A-type stars.—It is difficult to determine ages for A-type stars, but HR 7329 and HR 8799 appear to be young (<40 Myr) based on rotation, and more importantly, location on the H-R diagram. For massive stars, rotational velocities decline with age; HR 7329 (A0 V) has an especially large $v \sin i$ (330 km s^{-1}; Abt & Morrel 1995), which is considerably above the majority of early A-type stars ($\sim$100 km s^{-1}). HR 8799 (A5 V) has a moderate $v \sin i$ (40 km s^{-1}; Abt & Morrel 1995) and has been spectrally defined as a γ Bootis star (Gray & Kaye 1999), which implies an age of a few to 100 Myr. A color-luminosity relation of nearby young clusters (L00) seems to be correlated for stars of similar age; the 50–90 Myr IC 2391 and Alpha Per clusters lie below the older (600 Myr) Hyades and Praesepe. There is a large scatter in the Pleiades (70–125 Myr), which could be due to a range of distances and ages as well as unresolved binaries. HR 7329 and HR 8799 lie on a line located below the Alpha Per and IC 2391 clusters, which intersects β Pic, HR 4796, and HD 141569; this suggests that HR 7329 and HR 8799 are between 10 and 30 Myr old (L00). Finally, it has recently been suggested that HR 7329 is a member of a young comoving cluster (the Tucanae association) much like the TW Hydrae association with an age of $\sim$40 Myr (Zuckerman & Webb 2000; Webb 2000).

F-type stars.—HD 35850, HD 209253, and SAO 170610 are believed to be young (<0.3 Gyr) because of their rotation activity, lithium abundance, and X-ray activity. Tagliaferri et al. (1994) use the *Einstein* satellite to measure X-ray luminosities of $\log(L_{\rm X}) = 30.0$ and 29.7 ergs s^{-1} for HD 35850 and HD 209253, respectively. Late F- and G-type stars in the Pleiades typically have X-ray luminosities of $\log(L_{\rm X}) = 30$ ergs s^{-1}, while Hyades members fall under $\log(L_{\rm X}) = 29$ ergs s^{-1}.

Tagliaferri et al. (1994) find for HD 35850 and HD 209253 $v \sin i = 50$ and 16 km s^{-1} and $\log N({\rm Li}) = 3.2$ and 2.9, respectively, by fitting observations with synthetic model spectra.

These rotation velocities fall between those of Pleiades members and the UMa group. The positions of these two late F-type stars ($\log T_{\rm eff} \sim 3.8$) on a lithium versus $T_{\rm eff}$ plot is consistent with an age close to that of the Pleiades, but lithium ages for F-type stars are questionable and must be supported with other observations (Favata et al. 1993). The coronal activities (X-rays) and high rotational velocities are consistent with the lithium age of 100–200 Myr. SAO 170610 has a $\log N({\rm Li}) = 3.75$, which indicates a younger age, between the ages of the Taurus-Aurigae association and the Pleiades, or 20–125 Myr. There is also a small measured X-ray flux, $[\log(f_{\rm X}/f_v) = -4.15$; Stocke et al. 1991] consistent with a young age.

G-type stars.—Ten G-type stars were selected based on their chromospheric activity, lithium absorption, and rotation. The flux ratio of Ca II H and K emission to the bolometric flux, or $R'_{\rm HK}$, and lithium abundance, expressed $\log N({\rm Li})$, is compared among stars of young clusters. Henry et al. (1996) selected several stars as "very active" from Ca II emission, including HD 202917 ($\log R'_{\rm HK} = -4.06$) and HD 180445 ($\log R'_{\rm HK} = -3.90$). The Ca II H and K ratios imply ages for these objects, if these are single stars, similar to those of the Pleiades members, using the chromospheric emission-age relation of Donahue (1993):

$$\log(t) = 10.725 - 1.334 R_5 + 0.4085 R_5^2 - 0.0522 R_5^3, \quad (A1)$$

where t is age in Gyr, and R_5 is defined as $R'_{\rm HK} \times 10^5$. Soderblom et al. (1998b) measure a lithium abundance in HD 202917 $[\log N({\rm Li}) = 3.28]$ consistent with Pleiades stars of similar spectral type, but they measure only an upper limit $[\log N({\rm Li}) < 1.61]$ for HD 180445. Neither star rotates rapidly for G-type stars with $v \sin i = 12$ and 8 km s^{-1} for HD 202917 and HD 180445, respectively. Soderblom et al. (1998b) speculate that HD 180445 might be a spectroscopic binary. There is the hint of a second pair of spectral lines that could be a tidally locked secondary causing the chromospheric emission. Therefore, the age of HD 180445 is in question, but Soderblom et al. (1998b) conclude that HD 202917 is most likely a single, very active star that is younger than the Pleiades. Finally, Zuckerman & Webb (2000) suggest that HD 202917 is a member of the Tucanae association comoving cluster with an age of $\sim$40 Myr.

HD 105 was identified in Favata et al. (1995) as having a high lithium abundance $[\log N({\rm Li}) = 3.4]$. Using a distance determined by the *Hipparcos* mission, Favata et al. (1998) recomputed the X-ray flux density measured with the *Einstein* satellite and found $\log L_{\rm X} = 29.2$ ergs s^{-1}, which implies that HD 105 is a little younger than the Pleiades. For reference, the solar X-ray luminosity varies but is $\log L_{\rm X} \sim 27$ ergs s^{-1}. Jeffries (1995) lists a $v \sin i = 13$ km s^{-1} in his sample of active, lithium-rich stars.

Gl 311 (HD 72905) has a high level of chromospheric activity and rotates rapidly. Soderblom (1985) measure $\log R'_{\rm HK} = -4.7$, and Dorren & Guinan (1994) find a rotation period of 4.7 days, from which an age of 300 Myr could be assigned (Kirkpatrick et al. 2001). Recently, Gaidos et al. (2000) brought these data together with a lithium measure $[\log N({\rm Li}) = 2.8]$, derived (U, V, W) space motions ($+18.9$, $+12.1$, -3), and assessed that Gl 311 belonged to the UMa moving group ($+13$, $+1$, -8). From all indicators, it is evident that Gl 311 is most likely 0.3 Gyr old.

HD 220140 (V368 Cep) has been identified as an X-ray source with $\log L_{\rm X} = 30.5$ ergs s^{-1} (Pravdo et al. 1985), and light variations with a period of 2.75 days assumed to be due to spots have been measured (Heckert et al. 1990). Chugainov et al. (1991)

find no radial velocity variations over several nights, indicating a single star. They derive space motions of $(-22, -28, -4)$ that are marginally consistent with the Pleiades according to Eggen (1975; $-11, -25, -8$). They derive a lithium abundance of $\log N(\mathrm{Li}) = 3.0$ from their spectra and, based on these data, give an age of 0.05 Gyr, but it is probably closer to the Pleiades age of 0.125 Gyr from the rotational velocity. Therefore, we assign a range from 50 to 125 Myr.

It has been speculated that Gl 503.2 (HD 115043) is a member of the UMa comoving group, based on lithium abundance, kinematics, and chromospheric activity. Soderblom et al. (1993b) compared the abundances of lithium in several clusters and found Gl 503.2 to lie between the Hyades and Pleiades in abundances for G and K stars. The space velocities $(+15, +3, -8;$ Rocha-Pinto & Maciel 1998) are similar to the canonical UMa motions. Measurements of Ca II H and K lines ($\log R'_{\mathrm{HK}} = -4.43$) and rotational velocity ($v \sin i = 9$ km s^{-1}) were made by Soderblom & Mayor (1993). In a solar-like star, such activity is thought to be due to a youthful stage of high magnetic activity. When compared to other stars in Henry et al. (1996), the activity level places Gl 503.2 at less than 0.5 Gyr old, and it is listed with the most active stars in Soderblom et al. (1998a).

Gl 577 (HD 134319) has chromospheric emission in the Ca II H and K lines ($\log R'_{\mathrm{HK}} = -4.33$) that is similar to that of Pleiades stars (Henry et al. 1996), but its kinematic motions $(-33, -15, -1)$ are more consistent with the Hyades $(-40, -16, -3;$ Rocha-Pinto & Maciel 1998). Messina et al. (1998) ascertained a rotation period of 4.448 days from photometric variations thought to be due to dark spots on the surface. They note that this rotation period is about half that of most Hyades members, but it does correlate well with UMa group members (Dorren & Guinan 1994). Therefore, it might be as young as 300 Myr but could be as old as 600 Myr.

HD 70573 and RE 1507+76 are both listed in Jeffries (1995) as active, lithium-rich stars with $v \sin i = 11$ and 14 km s^{-1}, respectively, and lithium abundances above Pleiades values with lithium (6708 Å) equivalent widths (EWs) of 149 and 214 mÅ, respectively. Jeffries (1995) derives space motions of $(-41, -27, -18)$ and $(-14, -17, -11)$, respectively. The space motions of HD 70573 are inconsistent with those of Pleiades members, but from the lithium and rotation, we conclude that it is a little older than the Pleiades at 0.2 ± 0.1 Gyr. RE 1507+76 motions are closer to those of Pleiades members than those of either UMa or Hyades, consistent with the lithium abundance and rotation. We therefore assign an age of 0.1 Gyr.

HD 102982 was identified in Henry et al. (1996) as being a highly chromospherically active star because of emission in the Ca II H and K lines ($\log R'_{\mathrm{HK}} = -3.86$) giving an age less than the Pleiades. Mason et al. (1998) surveyed the most active stars listed in Henry et al. (1996) for multiplicity and found no companions to HD 102982 within 3 mag between $0''.035-1''.08$ using speckle techniques. Soderblom et al. (1998b) found HD 102982 to be a spectroscopic binary (SB2), and therefore the activity thought to result from youth might instead be caused by the close, less than a few AU, companion. This star ($b = 9°$) also slipped past our Galactic latitude requirement ($b > 15°$), because it was already on the observation calendar when the Galactic latitude cut was made.

The presence of the tidally locked companions to HD 102982 and HD 180445 places their ages in question. Our search with the coronagraph ($0''.5-4''$) covers $\sim 20-150$ AU at the distance of these stars (42 pc), so we did not expect to image a tidally locked companion but rather to search for a stable, lower mass companion farther out.

K-type stars.—HD 1405 was identified to have chromospheric emission (Bidelman 1985) and found to have a periodic variation ($P = 1.7$ days) of almost 0.1 mag, indicating rotation of cool spots (Griffin 1992). Pleiades members typically have rotation periods of a couple days. The radial velocity was found to remain constant, and that is consistent with the lack of a close companion. Fekel (1997) reports a $v \sin i = 23$ km s^{-1}, which agrees with 21 km s^{-1} of Griffin (1992). The rapid rotation and chromospheric emission with a lack of change in radial velocity are consistent with a youthful, single star at 0.1 Gyr.

HD 17925 is of particular interest because it is only 10 pc from the Sun. Favata et al. (1995) measured $\log N(\mathrm{Li}) = 2.88$ and $v \sin i < 8$ km s^{-1} in their sample of X-ray active stars. Henry et al. (1996) measured $v \sin i = 6$ km s^{-1} and find the Hα absorption partially filled in by emission, but they conclude that it could be a binary because of line-width variations seen over the three nights they observed. However, Abbott et al. (1995) report photometric modulation in a period of 7 days and a change in the light curve over a 3 week period consistent with a single, active star. The star has a large $\log R'_{\mathrm{HK}}$ (-4.30; Rocha Pinto & Maciel 1998), and Fekel (1997) measures space motions $(-14, -17, -11)$ close to that of the Pleiades, so we assign an age of 0.1–0.2 Gyr.

LkHα 264 was first identified as an emission-line star (Herbig & Rao 1972) and was later determined to be a classical T Tauri star still associated with the Lynds 1457 cloud at only 65 pc (Hobbs et al. 1986). Even though it is farther than 50 pc, it is likely a star that is a few million years old with an Hα EW of 100 mÅ (Gameiro et al. 1993). Using several lines of the spectrum, Gameiro et al. (1993) also measured a $v \sin i = 22$ km s^{-1} consistent with a young, late-type star.

HD 21703 was identified in the *Einstein* survey with a large X-ray flux [$\log(f_X/f_{\mathrm{bol}}) = -2.25$; Stocke et al. 1991], and Favata et al. (1995) measure an upper limit of $\log N(\mathrm{Li}) \leq 1.74$ and $v \sin i = 14$ km s^{-1}, placing this mid-K star near the Pleiades age from these indicators.

Three more K-type stars were selected from the Jeffries (1995) study of high-activity stars, correlating rotation and Hα emission with lithium abundance (Table A1). At this effective temperature, the gap between the Hyades lithium abundance and that of the Pleiades has widened significantly (Favata et al. 1993), and the ages of these objects are near the Pleiades age. RE 2131+23 and RE 0723+20 also have measured space motions of $(-4, -23, -13)$ and $(-6, -27, -15)$, very close to those of the Pleiades, supporting their young ages.

Henry et al. (1995) present results of photometric monitoring of HD 82443 deriving a period of 5.43 days, and they confirm it is single with a constant radial velocity. Fekel (1997) measured a $v \sin i = 6.2$ km s^{-1}, consistent with this earlier measurement. With a $\log R'_{\mathrm{HK}} = -4.20$ (Soderblom 1985) and space motions of $(-14, -24, -1)$ (Soderblom & Clements 1987), we conclude that this star is probably a little older than the Pleiades

TABLE A1
STARS FROM JEFFRIES (1995)

Star	Spectral Type	$v \sin i$ (km s^{-1})	Hα EW (mÅ)	Li EW (mÅ)	$\log N(\mathrm{Li})$[a]
RE 0041+34.....	K7	15	300	127	1.3
RE 0723+20.....	K5	12	350	105	1.2
RE 2131+23.....	K5	70	517	215	1.9

[a] Derived from lithium EW using Soderblom et al. (1993a).

TABLE A2
Active M Stars from Reid et al. (1995a)

Star	Spectral Type	Hα (Å)
Steph 932	M0.5	2.82
Gl 207.1	M2.5	7.98
PS 176........................	M3	7.37
LP 263-64	M3.5	7.83
LP 390-16	M4	10.05
GJ 1285......................	M4.5	16.37
LHS 2320....................	M5	14.47
LHS 2026....................	M6	21.13

age. Gl 354.1B is a wide (65″) proper motion companion to HD 82443, so we conclude that it is of a similar age and add it to our program under M-type stars.

HD 82558 is a chromospherically active, single star. Most main-sequence K-type stars are undetectable at radio frequencies, but Gudel (1992) detected a 3.6 cm flux of about 300 μJy and attributed it to gyrosynchrotron electrons in magnetic flux tubes in regions of high chromospheric activity. This star was selected for their study because of the X-ray emission (log L_X = 29.1 ergs s^{-1}) detected in the ROSAT All-Sky Survey. Jeffries (1995) lists $v \sin i$ = 25 km s^{-1}, lithium EW = 219 mÅ, and space motions of (−13, −5, −4) consistent with an age of <100 Myr.

Henry et al. (1995) found photometric variations in Gl 174 (HD 29697) with a period of 3.9 days, which they attribute to the presence of spots, deriving a $v \sin i$ = 7 km s^{-1}. They also measured a Hα EW of 200 mÅ and lithium EW of 79 mÅ. Using the conversion of Soderblom et al. (1993a), we convert this lithium measurement into an abundance of log N(Li) = 0.95. Eggen (1996) observed many low-mass stars and found photometric variations in Gl 174, correlated that with Ca II emission, and concluded that it was 60 Myr old. We conclude from the lithium abundance and chromospheric emission that it is probably closer to the Pleiades age, or about 100 Myr old.

Gl 517 (HD 118100) has a high X-ray flux density [log(L_X/L_{bol}) = −3.08; Sterzik & Schmitt 1997] typical of young stars approaching the main sequence, and Favata et al. (1997) measured log L_X = 29.54 ergs s^{-1}, which is consistent. EUV activity and flares were observed from Gl 517 (Tsikoudi & Kellett 1997). Favata et al. (1997) measured a lithium EW = 25 mÅ and rapid rotation and concluded that this star is a BY Dra that is a few tens of millions of years old.

Since Gl 879 (HD 216803) is the common proper motion companion to Fomalhaut, a well-studied A-type star with a debris disk (Holland et al. 1998; Staplefeldt et al. 2004), the determination of its age has been very important to disk formation theories. Barrado y Navascues et al. (1997) studied Gl 879 to determine the age of both components, placing several factors together. They note the lithium measure of log N(Li) = 0.6 makes the star younger than the Hyades but older than the Pleiades, while the X-ray activity (log L_X = 28.1; Favata et al. 1997) places the star's age closer to the Hyades age. The rotation ($v \sin i$ < 4 km s^{-1}) also places the star's age between those of the two clusters but more consistent with the younger Pleiades members, so they conclude an age of 200 ± 100 Myr for both Gl 879 and Fomalhaut.

Fekel (1997) finds HD 160934 has a constant radial velocity and a high $v \sin i$ (16.4 km s^{-1}). ROSAT detected this star with log(f_X/f_v) = −2.07 (Schachter et al. 1996), and Henry et al. (1995) measured photometric variability due to spots with a

period of ∼2 days. Therefore, from the rotation and chromospheric X-ray emission, it is most likely a Pleiades-age star.

HD 177996 was measured to have considerable Ca II emission (log R'_{HK} = −4.17; Henry et al. 1996), and Soderblom et al. (1998a) derived log N(Li) = 1.04, placing the star's age between the ages of the Hyades and the Pleiades. They do find it to be a double-lined spectroscopic binary, but they detect lithium in both stars and suggest an intermediate age of 0.5 Gyr.

Jeffries (1995) lists HD 197890 as a very active star with a $v \sin i$ = 170 km s^{-1} and log N(Li) = 3.1 (Anders et al. 1993). They derive space motions of (−6, −13, +1), similar to those of the Pleiades. Favata et al. (1998) measured X-ray activity (log L_X = 30.2) that is consistent with a 100 Myr old star.

M-type stars.—Usually, it is a little harder to determine an age for single M-type stars. For example, lithium is destroyed within a few million years in the fully convective interiors, and cooler surfaces tend to display a smaller amount of chromospheric activity. We list eight stars selected as the most active, single M-type stars from Reid et al. (1995a) in Table A2 and with higher than normal Hα activity, thought to be of Pleiades age (Fig. 9). The Hα EW ranges from 2 Å at M0 to 9 Å at M5 for the top 10% of Hyades members (Reid et al. 1995b) and from 4 Å at M0 to 12 Å at M5 for the same tier of Pleiades members (Hodgkin et al. 1995). Our targets are most consistent with the top members of the Pleiades cluster, suggesting ages of 100 Myr. Some M stars (<10%) have been observed to flare, and any of these measurements listed in Table A2 could have been taken during a flare. Therefore, we suggest that one should be cautious in determining ages from one observational criterion.

Gl 875.1 was detected in EUV flare activity (Tsikoudi & Kellett 1997), and Mathioudakis et al. (1995) measured a rotation period of 1.64 days and Hα EW of 3.9 Å. The rotation period is indicative of Pleiades-age stars, but the Hα is more consistent with an older star, perhaps UMa. Therefore, we assign an age of 0.2 Gyr.

TW Hydrae association.—Over the last few years mounting evidence has suggested that a number of young, active stars in the vicinity of TW Hydrae form a physical association with an age of ∼10 Myr (Kastner et al. 1997; Webb et al. 1999; Soderblom et al. 1998c). At an approximate distance of 60 pc, the TW Hydrae association (TWA) is the nearest region of recent star formation to the Sun (Kastner et al. 1997). Webb et al.

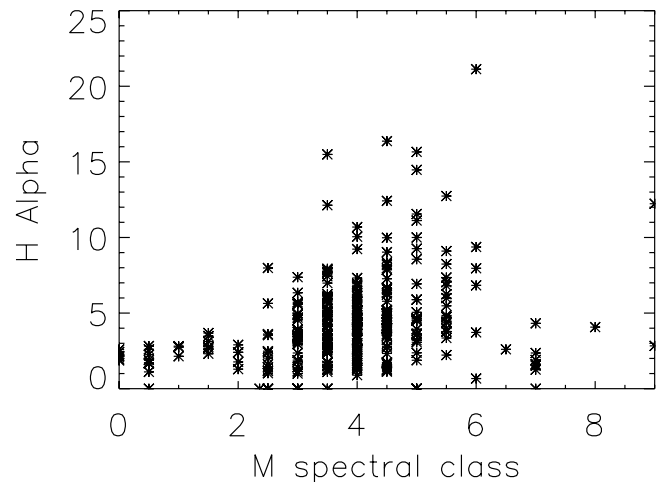

Fig. 9.—Hα measurement plotted against spectral type for those M-type stars with a measurement in Reid et al. (1995a). We took single targets from the top 10% of this distribution across all M spectral classes.

(1999) added HR 4796A and identified five new systems (seven members), in which each system is characterized by the presence of X-ray emission, Hα emission, and strong lithium absorption associated with young stars. The currently identified 11 systems are shown to have similar space motions, implying physical association and a possible common origin (Webb et al. 1999). We surveyed six of the members, TWA 1, 5, 6, 7, 8B, and 10, for possible brown dwarf companions. The multiple stars HR 4796A and HD 98800A/B were observed in a sister program for circumstellar disks.

REFERENCES

Abbott, B. P., Pomerance, B. H., & Ambruster, C. W. 1995, BAAS, 27, 842
Abt, H. A., & Morrell, N. I. 1995, ApJS, 99, 135
Anders, G. J., Jeffries, R. D., Kellett, B. J., & Coates, D. 1993, MNRAS, 265, 941
Bakos, G. A., Sahu, K. C., & Nemeth, P. 2002, ApJS, 141, 187
Baraffe, I., Chabrier, G., Allard, F., & Hauschildt, P. H. 1998, A&A, 337, 403
Barrado y Navascues, D., Stauffer, J. R., Hartmann, L., & Balachandran, S. C. 1997, ApJ, 475, 313
Bidelman, W. P. 1985, AJ, 90, 341
Bouvier, J., Rigaut, F., & Nadeau, D. 1997, A&A, 323, 139
Burgasser, A., Kirkpatrick, J. D., & Lowrance, P. 2005, AJ, 129, 2849
Burgasser, A., et al. 2002, ApJ, 564, 421
Burrows, A., Hubbard, W., Lunine, J., Marley, M., Huillot, T., Saumon, D., & Friedman, R. 1997, in ASP Conf. Ser. 119, Planets Beyond the Solar System and the Next Generation of Space Missions, ed. D. Soderblom (San Francisco: ASP), 9
Chugainov, P., Lovkaya, M., & Petrov, P. 1991, Inf. Bull. Variable Stars, 3623, 1
Donahue, R. A. 1993, Ph.D. thesis, New Mexico State Univ.
Dorren, J. D., & Guinan, E. F. 1994, ApJ, 428, 805
Duquennoy, A., & Mayor, M. 1991, A&A, 248, 485
Eggen, O. J. 1975, PASP, 87, 37
———. 1996, AJ, 111, 466
Favata, F., Barbera, M., Micela, G., & Sciortino, S. 1993, A&A, 277, 428
———. 1995, A&A, 295, 147
Favata, F., Micela, G., & Sciortino, S. 1997, A&A, 326, 647
Favata, F., Micela, G., Sciortino, S., & D'Antona, F. 1998, A&A, 335, 218
Fekel, F. 1997, PASP, 109, 514
Gaidos, E., Henry, G. W., & Henry, S. M. 2000, AJ, 120, 1006
Gameiro, J. F., Lago, M. T. V. T., Lima, N. M., & Cameron, A. C. 1993, MNRAS, 261, 11
Geballe, T. R., et al. 2002, ApJ, 564, 466
Gizis, J., Kirkpatrick, J. D., Burgasser, A., Reid, I. N., Monet, D. G., & Liebert, J. 2001, ApJ, 551, L163
Gray, R. O., & Kaye, A. B. 1999, AJ, 118, 2993
Griffin, R. F. 1992, Observatory, 112, 41
Gudel, M. 1992, A&A, 264, L31
Guenther, E. W., Neuhauser, R., Huelamo, N., Brandner, W., & Alves, J. 2001, A&A, 365, 514
Harrington, R. S. 1977, AJ, 82, 753
Hayward, T. L., Brandl, B., Pirger, B., Blacken, C., Gull, G. E., Schoenwald, J., & Houck, J. R. 2001, PASP, 113, 105
Heckert, P. A., Mooney, C. B., Hickman, M. A., & Summers, D. 1990, BAAS, 22, 837
Henry, G. W., Fekel, F., & Hall, D. 1995, AJ, 110, 2926
Henry, T. J., Soderblom, D. R., Donahue, R. A., & Baliunas, S. L. 1996, AJ, 111, 439
Herbig, G. H., & Rao, N. K. 1972, ApJ, 174, 401
Hobbs, L. M., Blitz, L., & Magnani, L. 1986, ApJ, 306, L109
Hodapp, K. W., et al. 1994, Proc. SPIE, 2198, 668
Hodgkin, S. T., Jameson, R. F., & Steele, I. A. 1995, MNRAS, 274, 869
Høg, E., et al. 2000, A&A, 355, L27
Holland, W. S., et al. 1998, Nature, 392, 788
Jeffries, R. 1995, MNRAS, 273, 559
Kastner, J. H., Zuckerman, B., Weintraub, D. A., & Forveille, T. 1997, Science, 277, 67
Kirkpatrick, J. D., Dahn, C. C., Monet, D. G., Reid, I. N., Gizis, J., Liebert, J., & Burgasser, A. 2001, AJ, 121, 3235
Kirkpatrick, J. D., Henry, T., & Irwin, M. J. 1997, AJ, 113, 1421
Kirkpatrick, J. D., Henry, T., & McCarthy, D. W. 1991, ApJS, 77, 417
Kirkpatrick, J. D., et al. 1999, ApJ, 519, 802
Koerner, D., Kirkpatrick, J. D., McElwain, M., & Bonaventura, N. R. 1999, ApJ, 526, L25
Krist, J. E., & Hook, R. N. 1997, in The 1997 HST Calibration Workshop with a New Generation of Instruments, ed. S. Casertano et al. (Baltimore: STScI), 192
Leggett, S. K., Allard, F., Berriman, G., Dahn, C. C., & Hauschildt, P. H. 1996, ApJS, 104, 117
Leggett, S. K., Allard, F., & Hauschildt, P. H. 1998, ApJ, 509, 836
Lin, D. N. C., & Ida, S. 1997, ApJ, 477, 781

Lowrance, P. J., et al. 1999, ApJ, 512, L69 (L99)
———. 2000, ApJ, 541, 390 (L00)
Luhman, K. L., & Rieke, G. H. 1998, ApJ, 497, 354
Luyten, W. 1979, LHS Catalogue: A Catalogue of Stars with Proper Motions Exceeding 0″5 Annually (2nd ed.; Minneapolis: Univ. Minnesota)
MacKenty, J. W., et al. 1997, NICMOS Instrument Handbook, Ver. 2.0 (Baltimore: STScI)
Marcy, G. W., Butler, R. P., Fischer, D. A., & Vogt, S. S. 2004, in ASP Conf. Proc. 321, Extrasolar Planets: Today and Tomorrow, ed. J.-P. Beaulieu, A. Lecavelier des Etangs, & C. Terquem (San Francisco: ASP), 3
Mason, B. D., Henry, T. J., Hartkopf, W. I., ten Brummelaar, T., & Soderblom, D. R. 1998, AJ, 116, 2975
Mathioudakis, M., Fruscione, A., Drake, J. J., McDonald, K., Bowyer, S., & Malina, R. F. 1995, A&A, 300, 775
Mayor, M., & Queloz, D. 1995, Nature, 378, 355
McLean, I. S., et al. 1998, Proc. SPIE, 3354, 566
McLeod, B. 1997, in The 1997 HST Calibration Workshop with a New Generation of Instruments, ed. S. Casertano et al. (Baltimore: STScI), 281
Messina, S., Guinan, E. F., & Lanza, A. 1998, Ap&SS, 260, 493
Montes, D., López-Santiago, J., Galvez, M. C., Fernández-Figueroa, M. J., De Castro, E., & Cornide, M. 2001, MNRAS, 328, 45
Mugrauer, M., et al. 2004, A&A, 417, 1031
Nakajima, T., Oppenheimer, B. R., Kulkarni, S. R., Golimowski, D. A., Matthews, K., & Durrance, S. T. 1995, Nature, 378, 463
Neuhäuser, R., Brandner, W., Eckart, A., Guenther, E., Alves, J., Ott, T., Huélamo, N., & Fernández, M. 2000a, A&A, 354, L9
Neuhäuser, R., Guenther, E. W., Petr, M. G., Brandner, W., Huélamo, N., & Alves, J. 2000b, A&A, 360, L39
Patience, J., Ghez, A. M., Reid, I. N., & Matthews, K. 2002, AJ, 123, 1570
Patience, J., Ghez, A. M., Reid, I. N., Weinberger, A. J., & Matthews, K. 1998, AJ, 115, 1972
Perryman, M. A. C., et al. 1997, A&A, 323, L49
Pravdo, S. H., White, N. E., & Giommi, P. 1985, MNRAS, 215, 11P
Rebolo, R., Zapatero Osorio, M. R., & Martin, E. L. 1995, Nature, 377, 129
Reid, I. N. 1999, in Proc. Star Formation 1999, ed. T. Nakamoto (Nagoya: Nobeyama Radio Obs.), 327
Reid, I. N., Gizis, J., Kirkpatrick, J. D., & Koerner, D. 2001, AJ, 121, 489
Reid, I. N., Hawley, S., & Gizis, J. 1995a, AJ, 110, 1838
Reid, I. N., Hawley, S., & Mateo, M. 1995b, MNRAS, 272, 828
Rigaut, F., et al. 1998, PASP, 110, 152
Rocha-Pinto, H. J., & Maciel, W. J. 1998, MNRAS, 298, 332
Schachter, J., Remillard, R., Saar, S. H., Favata, F., Sciortino, S., & Barbera, M. 1996, ApJ, 463, 747
Schneider, G. 1998, in ESO Conf. Proc. 55, NICMOS and the VLT: A New Era of High Resolution Near Infrared Imaging and Spectroscopy, ed. W. Freudling & R. Hook (Garching: ESO), 88
———. 2002, in The 2002 HST Calibration Workshop, ed. S. Arribas, A. Koekemoer, & B. Whitmore (STScI: Baltimore), 250
Schneider, G., Becklin, E. E., Smith, B. A., Hines, D., Weinberger, A. J., & Silverstone, M. 2001, AJ, 121, 525
Skrutskie, M., et al. 1997, in The Impact of Large Scale Near-IR Sky Surveys, ed. F. Garzon et al. (Dordrecht: Kluwer), 25
Soderblom, D. R. 1985, AJ, 90, 2103
Soderblom, D. R., & Clements, S. 1987, AJ, 93, 920
Soderblom, D. R., Jones, B., Balachandran, S., Stauffer, J. R., Duncan, D., Fedele, S., & Hudon, J. D. 1993a, AJ, 106, 1059
Soderblom, D. R., King, J., Hanson, R., Jones, B., Fischer, D., Stauffer, J. R., & Pinsonneault, M. 1998a, ApJ, 504, 192
Soderblom, D. R., King, J., & Henry, T. 1998b, AJ, 116, 396
Soderblom, D. R., & Mayor, M. 1993, AJ, 105, 226
Soderblom, D. R., Pilachowski, C., Fedele, S., & Jones, B. 1993b, AJ, 105, 2299
Soderblom, D. R., et al. 1998c, ApJ, 498, 385
Staplefeldt, K., et al. 2004, ApJS, 154, 458
Stauffer, J. R., Schultz, G., & Kirkpatrick, J. D. 1998, ApJ, 499, L199
Sterzik, M. F., & Schmitt, J. 1997, AJ, 114, 1673
Stocke, J. T., Morris, S., Gioia, I. M., Maccacaro, T., Schild, R., Wolter, R., Fleming, T., & Henry, J. P. 1991, ApJS, 76, 813

No. 4, 2005   CORONAGRAPHIC SURVEY FOR SUBSTELLAR COMPANIONS   1861

Tagliaferri, G., et al. 1994, A&A, 285, 272

Thompson, R., Rieke, M., Schneider, G., Hines, D., & Corbin, M. 1998, ApJ, 492, L95

Tsikoudi, V., & Kellett, B. J. 1997, MNRAS, 285, 759

Webb, R. A. 2000, Ph.D. thesis, UCLA

Webb, R. A., Zuckerman, B., White, R. J., Patience, J., Schwartz, M., McCarthy, C., & Platais, I. 1999, ApJ, 512, L63

Weiss, E. 1991, AJ, 101, 1882

York, D. G., et al. 2000, AJ, 120, 1579

Zapatero Osorio, M. R., Martin, E. L., & Rebolo, R. 1997a, A&A, 323, 105

Zapatero Osorio, M. R., Rebolo, R., Martin, E. L., Basri, G., Magazzu, A., Hodgkin, S. T., Jameson, R. F., & Cossburn, M. R. 1997b, ApJ, 491, L81

Zuckerman, B., & Webb, R. A. 2000, ApJ, 535, 959